Molecular Road Map to Tuning Ground State Absorption and Excited State Dynamics of Long-Wavelength Absorbers

Yusong Bai,[a] Jean-Hubert Olivier,[a] Hyejin Yoo,[a] Nicholas F. Polizzi,[a] Jaehong Park,[a,b] Jeff Rawson,[a] and Michael J. Therien[a*]

[a]Department of Chemistry, French Family Science Center, 124 Science Drive, Duke University, Durham, North Carolina 27708-0346, USA

[b]Department of Chemistry, University of Pennsylvania, 231 South 34th Street, Philadelphia, PA 19104-6323, USA

Contents

1. Materials and Instrumentation

Materials. All manipulations were carried out under nitrogen or argon previously passed through an O_2 scrubbing tower (Schweitzerhall R3-11 catalyst) and a drying tower (Linde 3-Å molecular sieves) unless otherwise stated. Air sensitive solids were handled in a Braun 150-M glove box. Standard Schlenk techniques were employed to manipulate air-sensitive solutions. All solvents utilized in this work were obtained from Fisher Scientific (HPLC Grade). CH_2Cl_2 and tetrahydrofuran (THF) were distilled from CaH_2 and K/4-benzoylbiphenyl, respectively, under argon. Triethylamine (TEA) was dried over KOH pellets and distilled under vacuum. All NMR solvents were used as received. The catalysts $Pd(PPh_3)_4$ and tris(dibenzylideneacetone)-dipalladium(0) (Pd_2dba_3), as well as triphenylarsine ($AsPh_3$),were purchased from Sigma-Aldrich. Various starting materials (Scheme S1), such as ruthenium(II) (4'-bromo-2,2';6',2"-terpyridine)(4'-pyrrolidin-1-yl- 2,2';6',2"-terpyridine) bis(hexafluorophosphate) (**Pyr_1RuBr**),[1] osmium(II) (4'-bromo-2,2';6',2"-terpyridine)(2,2';6',2"-terpyridine) bis(hexafluorophosphate) (**OsBr**),[1e,2] [5,15-bis-ethynyl-10,20-bis(2',6'-bis(3,3-dimethyl-1-butyloxy)phenyl)porphinato]zinc(II) (**EPZnE**),[2a,3] 1,2-bis[(10,20-bis(2',6'-bis(3,3-dimethyl-1-butyloxy)phenyl)porphinato)zinc(II)]ethyne (**PZn_2**)[3-4] were prepared according to the published procedures. Flash and size exclusion column chromatography were performed on the bench top, using respectively silica gel (EM Science, 230–400 mesh) and Bio-Beads SX-1 as media.

Instrumentation. Electronic spectra were recorded on a Varian 5000 UV/vis/NIR spectrophotometry system. NMR spectra were recorded on a 400 MHz AC-Brucker instrument. Chemical shifts for ^{1}H NMR spectra are reported relative to residual protium in the deuterated solvents ($CDCl_3$ = 7.26 ppm, CD_3CN = 1.93 ppm). All J values are reported in Hertz. MALDI-TOF mass spectroscopic data were obtained with a Perspective Voyager DE Instrument (Department of Chemistry, Duke University). Samples were prepared as micromolar solutions in acetone, and 2-(4'-hydroxybenzeneazo)benzoic acid (Sigma-Aldrich) was utilized as the matrix. Microwave assisted reactions were performed with Emrys Personal Chemistry System (Biotage).

2. Synthetic Procedures and Characterization of New Chromophores

Discussion of General Synthetic Strategies. Pyr$_1$RuPZnRuPyr$_1$ was synthesized by cross-coupling of **Pyr$_1$RuBr** with [5,15-bis(ethynyl)-10,20-bis(2',6'-bis(3,3-dimethyl-1-butyloxy)phenyl)porphinato]zinc(II) (Scheme 1). **Pyr$_1$RuPZn$_2$RuPyr$_1$**, **OsPZn$_2$Os**, **Pyr$_1$RuPPt$_2$RuPyr$_1$**, **Pyr$_1$RuPZnPPtPZnRuPyr$_1$** and **Pyr$_1$RuPZnPPdPZnRuPyr$_1$** were prepared in a similar fashion, cross-coupling bis(*meso*-ethynyl) ethyne-bridged oligo(porphinato)metal(II) species (**EPZn$_2$E**, **EPPt$_2$E**, **EPZnPPtPZnE** and **EPZnPPdPZnE**) with either **Pyr$_1$RuBr** or **OsBr** (Scheme 1). Overall yields (based on the **10,20-bis(2',6'-bis(3,3-dimethyl-1-butyloxy)phenyl)porphyrin** starting material) for the final products are outlined in Scheme S7.

Synthetic Procedures.

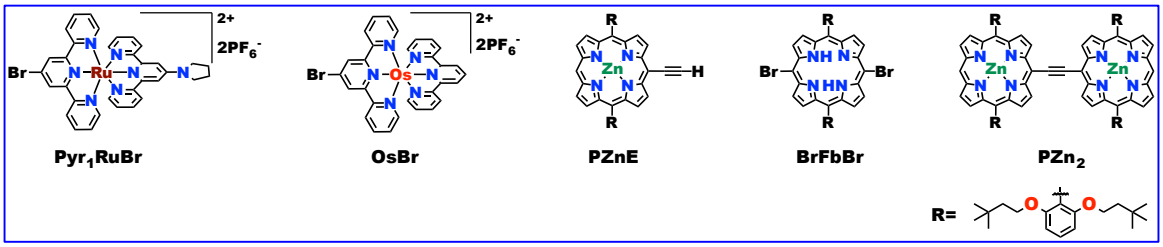

Scheme S1. Precursor compounds utilized for the synthesis of ethyne-bridged oligo(porphinato)metal(II)-bis(terpyridyl)metal(II) chromophores; these compounds were prepared according to previously published procedures (see Materials section above).

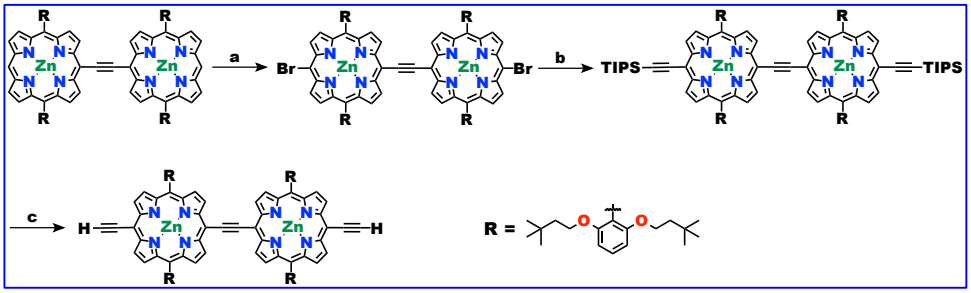

Scheme S2. Synthesis of **EPZn$_2$E** from **PZn$_2$**. (a) NBS, 0 ^{o}C, CH_2Cl_2:pyridine 20:1 mixture, 1.5 h, under argon; (b) (triisopropylsilyl)acetylene, $Pd(PPh_3)_2Cl_2$, CuI, THF:*i*-Pr_2NH 9:1 mixture, 60 ^{o}C, 16 h, under argon; (c) TBAF, THF, 0 ^{o}C, 10 min, under argon.

1,2-Bis[(5-bromo-10,20-bis(2',6'-bis(3,3-dimethyl-1-butyloxy)phenyl)porphinato)zinc(II)]ethyne (BrPZn$_2$Br). In a 500 mL round bottom flask, **PZn$_2$** (448 mg, 0.24 mmol) was dissolved in methylene chloride (100 mL) and pyridine (10 mL).

The reaction mixture was cooled to 0 °C and a solution of NBS (90 mg, 0.50 mmol) in methylene chloride (100 mL) was added via cannula. The reaction mixture was stirred at 0 °C under argon for 1.5 h and quenched by addition of H_2O (100 mL). The organic layer was separated and dried with anhydrous Na_2SO_4. After evaporation of the solvent, the residue was purified by column chromatography using 1:1 hexanes:methylene chloride as the eluent. Yield = 440 mg (90 %, based on 448 mg of the **PZn$_2$** starting material). ^{1}HNMR (400MHz, $CDCl_3$ as 7.26 ppm): δ 10.33 (d, 4H, J = 4.4 Hz), 9.61 (d, 4H, J = 4.8), 9.02 (d, 4H, J = 4.4 Hz), 8.86 (d, 4H, J = 4.4 Hz), 7.74 (t, 4H, J = 8.4 Hz), 7.05 (d, 8H, J = 8.4 Hz), 3.96 (t, 16H, J = 7.4 Hz), 0.90 (t, 16H, J = 7.4 Hz), 0.36 (s, 72H). MALDI-TOF: m/z = 2033.02 (calculated for $C_{114}H_{132}Br_2N_8O_8Zn_2$ $(M+H)^+$ 2031.93).

1,2-Bis[(5-triisopropylsilylethynyl-10,20-bis(2',6'-bis(3,3-dimethyl-1-butyloxy)phenyl)porphinato)zinc(II)]ethyne (TIPS-EPZn$_2$E-TIPS). A 100 mL Schlenk flask equipped with a magnetic stirbar was charged with **BrPZn$_2$Br** (440 mg, 0.22 mmol), $Pd(PPh_3)_2Cl_2$ (32 mg, 0.044 mmol) and CuI (10 mg, 0.044 mmol). A solvent mixture of THF (50 mL), diisopropylamine (5ml), and (triisopropylsilyl)acetylene (400 µL, 1.30 mmol) was degassed via three-pump-thaw cycles, transferred to the reaction flask and stirred at 60 °C for 16 h. After the reaction endpoint was confirmed by TLC, the reaction mixture was poured into water, extracted with CH_2Cl_2, dried over Na_2SO_4, and evaporated. The residue was purified by column chromatography using 1:1 hexanes:methylene chloride as the eluent. Yield = 360 mg (75%, based on 220 mg of **BrPZn$_2$Br**). ^{1}H NMR (400MHz, $CDCl_3$ as 7.26 ppm): δ 10.35 (d, 4H, J = 4.8 Hz), 9.73 (d, 4H, J = 4.4), 9.07 (d, 4H, J = 4.4 Hz), 8.94 (d, 4H, J = 4.4 Hz), 7.77 (t, 4H, J = 8.4 Hz), 7.08 (d, 8H, J = 8.4 Hz), 4.01 (t, 16H, J = 7.2 Hz), 1.55-1.49 (m, 42H), 0.97 (t, 16H, J = 7.4 Hz), 0.37 (s, 72H). MALDI-TOF: m/z = 2235.65 (calculated for $C_{136}H_{174}N_8O_8Si_2Zn_2$ $(M+H)^+$ 2234.87).

1,2-Bis[(5-ethynyl-10,20-bis(2',6'-bis(3,3-dimethyl-1-butyloxy)phenyl)porphinato)zinc(II)]ethyne (EPZn$_2$E). Tetrabutylammonium fluoride (1 M in THF, 220 µL, 0.22 mmol) was added to a solution of **TIPS-EPZn$_2$E-TIPS** (200 mg, 0.089 mmol) in THF (50 ml) under argon at 0 °C. The reaction mixture was stirred for 10 min at 0 °C, quenched with water, extracted with CH_2Cl_2, dried over Na_2SO_4, and evaporated. The residue was chromatographed on silica gel using 1:1 hexanes:methylene chloride as the eluent. Yield =

166 mg (97%, based on 137 mg of **TIPS-EPZn$_2$E-TIPS**). ^{1}H NMR (400MHz, $CDCl_3$ as 7.26 ppm): δ 10.34 (d, 4H, J = 4.8 Hz), 9.72 (d, 4H, J = 4.4), 9.04 (d, 4H, J = 4.4 Hz), 8.92 (d, 4H, J = 4.4 Hz), 7.74 (t, 4H, J = 8.4 Hz), 7.06 (d, 8H, J = 8.4 Hz), 4.13 (s, 2H), 3.98 (t, 16H, J = 7.2 Hz), 0.93 (t, 16H, J = 7.4 Hz), 0.36 (s, 72H). MALDI-TOF: m/z = 1921.56 (calculated for $C_{118}H_{134}N_8O_8Zn_2$ $(M+H)^+$ 1923.18).

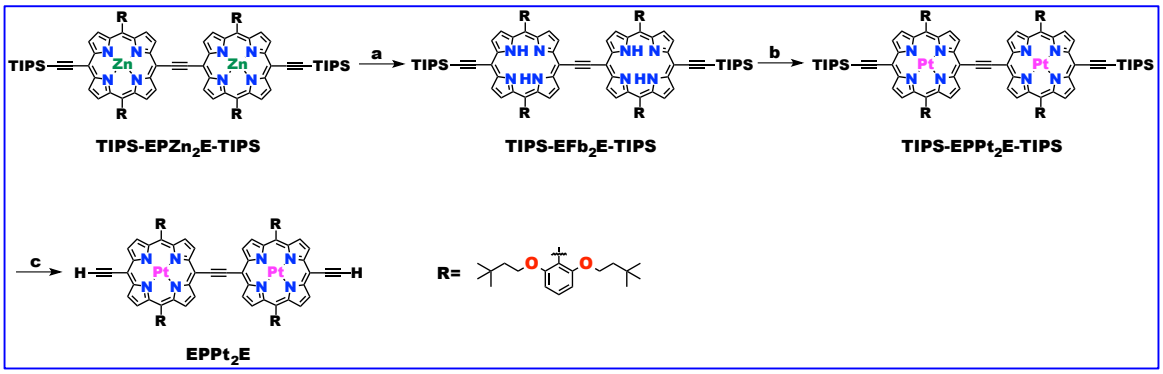

Scheme S3. Synthesis of **EPPt$_2$E** from **TIPSEPZn$_2$ETIPS**. (a) trifluoroacetic acid, r.t., CH_2Cl_2, 30 min; (b) $Pt(acac)_2$, benzonitrile, 200 ^oC, 4 h, microwave reaction; (c) TBAF, THF, 0 ^oC, 10 min, under argon.

1,2-Bis(5-triisopropylsilylethynyl-10,20-bis(2',6'-bis(3,3-dimethyl-1-butyloxy)phenyl)porphyryl)ethyne (TIPS-EFb$_2$E-TIPS). In a 100 mL round bottom flask equipped with a magnetic stirring bar, **TIPS-EPZn$_2$E-TIPS** (120 mg, 0.054 mmol) was dissolved by dry methylene chloride (~50 mL). Trifluoroacetic acid (1 mL) was added to the round bottom flask and the reaction was stirred at room temperature under argon for 0.5 h and then quenched by saturated $NaHCO_3$. The organic layer was collected, washed with saturated NH_4Cl, and then dried with Na_2SO_4. After evaporation of the solvent, the residue was purified by column chromatography using 1:1 hexanes:methylene chloride as the eluent. Yield = 112 mg (98 %, based on 120 mg of the **TIPS-EPZn$_2$E-TIPS** starting material). ^{1}H NMR (400MHz, $CDCl_3$ as 7.26 ppm): δ 10.22 (d, 4H, J = 4.8 Hz), 9.62 (d, 4H, J = 4.4), 8.97 (d, 4H, J = 4.8 Hz), 8.85 (d, 4H, J = 4.8 Hz), 7.77 (t, 4H, J = 8.4 Hz), 7.07 (d, 8H, J = 8.4 Hz), 4.00 (t, 16H, J = 7.2 Hz), 1.55-1.49 (m, 42H), 0.99 (t, 16H, J = 7.4 Hz), 0.40 (s, 72H), -1.94 (s, 4H). MALDI-TOF: m/z = 2106.28 (calculated for $C_{136}H_{178}N_8O_8Si_2$ $(M+H)^+$ 2109.14).

1,2-Bis[(5-triisopropylsilylethynyl-10,20-bis(2',6'-bis(3,3-dimethyl-1-butyloxy)phenyl)porphinato)platinum(II)]ethyne (TIPS-EPPt$_2$E-TIPS). TIPS-EFb$_2$E-TIPS (70 mg, 0.033 mmol), platinum acetylacetonate (129 mg, 0.33 mmol) and a magnetic stirring bar

were brought together into a 10 mL microwave reaction vial that was then sealed and charged with argon. These reagents were dissolved in ~6 mL of benzonitrile solvent that was previously purged with argon for 1 h. The reaction vial was stirred at 200 ^{o}C for 4 h in a microwave irradiation cavity. After the reaction, without removing the benzonitrile solvent, the reaction mixture was directly purified via silica column chromatography using 65:35 hexanes:methylene chloride eluent, and the first greenish band was collected as the desired product. Yield = 50 mg (61%, based on 70 mg of the **TIPS-EFb$_2$E-TIPS** starting material). ^{1}H NMR (400MHz, $CDCl_3$ as 7.26 ppm): δ 10.08 (d, 4H, J = 5.2 Hz), 9.55 (d, 4H, J = 5.2), 8.87 (d, 4H, J = 5.2 Hz), 8.77 (d, 4H, J = 5.2 Hz), 7.71 (t, 4H, J = 8.4 Hz), 7.02 (d, 8H, J = 8.8 Hz), 3.97 (t, 16H, J = 7.2 Hz), 1.49-1.44 (m, 42H), 0.98 (t, 16H, J = 7.2 Hz), 0.31 (s, 72H). MALDI-TOF: m/z = 2491.96 (calculated for $C_{136}H_{174}N_8O_8Si_2Pt_2$ $(M+H)^+$ 2495.27).

1,2-Bis[(5-ethynyl-10,20-bis(2',6'-bis(3,3-dimethyl-1-butyloxy)phenyl)porphinato)platinum(II)]ethyne (EPPt$_2$E). Tetrabutylammonium fluoride (1 M in THF, 50 µL, 0.050 mmol) was added to a solution of **TIPS-EPPt$_2$E-TIPS** (50 mg, 0.020 mmol) in THF (30 ml) under argon at 0 °C. The reaction mixture was stirred for 10 min at 0 °C, quenched with water, extracted with CH_2Cl_2, dried over Na_2SO_4, and evaporated. The residue was chromatographed on silica gel using 85:15 hexanes:THF as the eluent. Yield = 41 mg (95%, based on 50 mg of **TIPS-EPPt$_2$E-TIPS**). ^{1}H NMR (400MHz, $CDCl_3$ as 7.26 ppm): δ 10.05 (d, 4H, J = 5.2 Hz), 9.54 (d, 4H, J = 5.2), 8.88 (d, 4H, J = 5.2 Hz), 8.76 (d, 4H, J = 5.2 Hz), 7.71 (t, 4H, J = 8.4 Hz), 7.02 (d, 8H, J = 8.8 Hz), 4.09 (s, 2H), 3.96 (t, 16H, J = 7.2 Hz), 1.49-1.45 (m, 42H), 0.96 (t, 16H, J = 7.2 Hz), 0.32 (s, 72H). MALDI-TOF: m/z = 2179.64 (calculated for $C_{118}H_{134}N_8O_8Pt_2$ $(M+H)^+$ 2182.59).

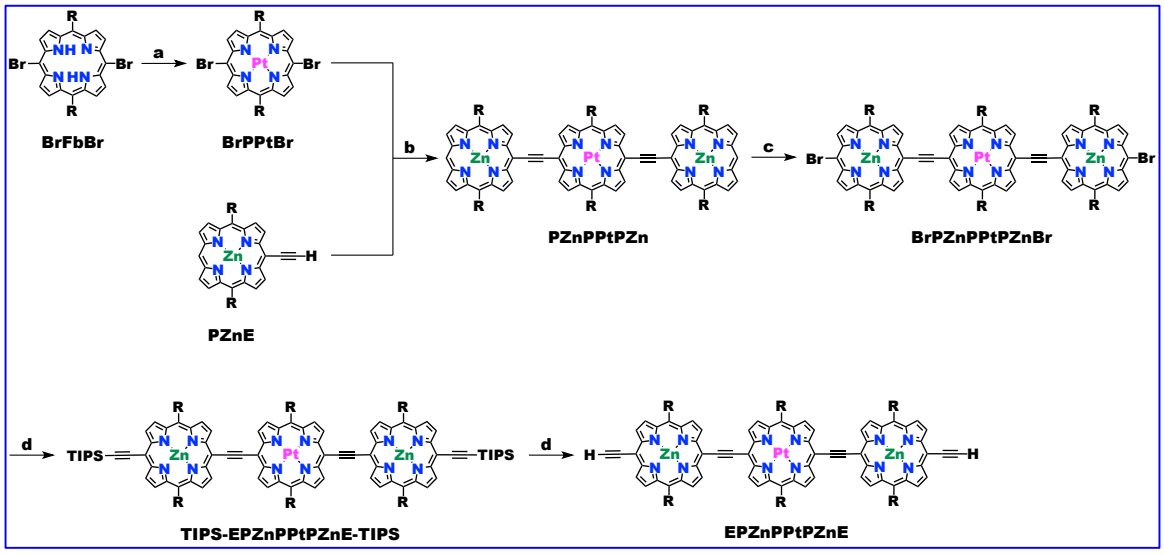

Scheme S4. Synthesis of **EPZnPPtPZnE**. (a) $Pt(acac)_2$, benzonitrile, 200 ^oC, 4 h, microwave reaction; (b) $Pd_2(dba)_3$, $AsPh_3$, THF:*i*-Pr_2NH 9:1 mixture, 50 ^oC, 12 h, under argon; (c) NBS, 0 ^oC, CH_2Cl_2:pyridine 20:1 mixture, 1.5 h, under argon; (d) (triisopropylsilyl)acetylene, $Pd(PPh_3)_2Cl_2$, CuI, THF:*i*-Pr_2NH 9:1 mixture, 60 ^oC, 16 h, under argon; (e) TBAF, THF, 0 ^oC, 10 min, under argon.

[5,15-Dibromo-10,20-bis(2',6'-bis(3,3-dimethyl-1-butyloxy)phenyl)porphinato]platinum(II) (BrPPtBr). BrFbBr (70 mg, 0.069 mmol), platinum acetylacetonate (135 mg, 0.34 mmol) and a magnetic stirring bar were brought together into a 10 mL microwave reaction vial that was then sealed and charged with argon. These reagents were dissolved in 6 mL of benzonitrile solvent that was previously purged with argon for 1 h. The reaction vial was stirred at 200 ^oC for 4 h in a microwave irradiation cavity. After the reaction, without removing the benzonitrile solvent, the reaction mixture was directly purified by silica column chromatography using 65:35 hexanes:methylene chloride eluent; the first bright orange color band was collected as the desired product. This reaction was repeated three additional times in order to obtain enough material for subsequent reactions. Yield = 271 mg (products from 4 reactions in total, 81%, based on 280 mg of the **BrFbBr** starting material). ^1H NMR (400MHz, $CDCl_3$ as 7.26 ppm): δ 9.52 (dd, 4H, J = 5.2 Hz, 0.8 Hz), 8.77 (d, 4H, J = 5.2 Hz, 0.8 Hz), 7.73 (t, 2H, J = 8.4 Hz), 7.02 (d, 4H, J = 8.0 Hz), 3.95 (t, 8H, J = 7.2 Hz), 0.95 (t, 8H, J = 7.2 Hz), 0.29 (s, 36H). MALDI-TOF: m/z = 1212.84 (calculated for $C_{56}H_{66}N_4O_4Br_2Pt$ $(M+H)^+$ 1214.06).

5,15-Bis[5'-[[10', 20'-bis(3,5-di(3,3-dimethyl-1-butyloxy)phenyl)porphinato]zinc(II)]ethynyl]-[10,20-bis(2',6'-bis(3,3-dimethyl-1-

butyloxy)phenyl)porphinato]platinum(II) (PZnPPtPZn). A 100 mL Schlenk flask equipped with a magnetic stirbar was charged with **PZnE** (370 mg, 0.39 mmol), **BrPPtBr** (190 mg, 0.16 mmol), $Pd_2(dba)_3$ (36 mg, 0.039 mmol) and $AsPh_3$ (48 mg, 0.156 mmol). A solvent mixture of THF (50 mL) and diisopropylamine (5 ml) was degassed via five freeze-pump-thaw cycles, transferred to the reaction flask, and stirred at 50 °C for 12 h. After the reaction endpoint was confirmed by TLC, the reaction mixture was evaporated to dryness and the residue sequentially purified by silica column chromatography using 1:1 hexanes:methylene chloride as the eluent, size exclusion column chromatography using THF as the eluent, and an additional silica column chromatographic step using 1:1 hexanes:methylene chloride as the eluent. Yield = 218 mg (46%, based on 190 mg of **BrPPtBr**). ^{1}H NMR (400MHz, $CDCl_3$ as 7.26 ppm): δ 10.38 (d, 4H, J = 4.4 Hz), 10.24 (d, 4H, J = 5.2), 10.11 (s, 2H), 9.29 (d, 4H, J = 4.4 Hz), 9.15 (d, 4H, J = 4.4 Hz), 9.00 (d, 4H, J = 4.4 Hz), 8.94 (d, 4H, J = 5.2 Hz), 7.76 (t, 4H, J = 8.4 Hz), 7.75 (t, 2H, J = 8.4), 7.08 (d, 8H, J = 8.4 Hz), 7.07 (d, 4H, J = 8.8 Hz), 4.04 (t, 8H, J = 7.2 Hz), 3.98 (t, 16H, J = 7.2 Hz), 1.06 (t, 8H, J = 7.2 Hz), 0.93 (t, 16H, J = 7.2 Hz), 0.35 (s, 36H), 0.31 (s, 72H). MALDI-TOF: m/z = 2957.32 (calculated for $C_{172}H_{200}N_{12}O_{12}PtZn_2$ $(M+H)^+$ 2953.41).

5,15-Bis[5'-[[15'-bromo-10', 20'-bis(3,5-di(3,3-dimethyl-1-butyloxy)phenyl)porphinato]zinc(II)]ethynyl]-[10,20-bis(2',6'-bis(3,3-dimethyl-1-butyloxy)phenyl)porphinato]platinum (II) (BrPZnPPtPZnBr). In a 250 mL round bottom flask, **PZnPPtPZn** (180 mg, 0.061 mmol) was dissolved in methylene chloride (50 mL) and pyridine (5 mL). The reaction mixture was cooled to 0 °C and a solution of NBS (22 mg, 0.13 mmol) in methylene chloride (50 mL) was added via cannula. The reaction mixture was stirred at 0 °C under argon for 1.5 h and quenched by addition of H_2O (100 mL). The organic layer was separated and dried with anhydrous Na_2SO_4. After evaporation of the solvent, the residue was purified by column chromatography using 6:4 hexanes:methylene chloride as the eluent. Yield = 127 mg (67 %, based on 180 mg of the **PZnPPtPZn** starting material). ^{1}H NMR (400MHz, $CDCl_3$ as 7.26 ppm): δ 10.27 (d, 4H, J = 4.8 Hz), 10.20 (d, 4H, J = 4.8), 9.63 (d, 4H, J = 4.8 Hz), 9.03 (d, 4H, J = 4.4 Hz), 8.92 (d, 4H, J = 5.2 Hz), 8.88 (d, 4H, J = 4.8 Hz), 7.75 (t, 6H, J = 8.4 Hz), 7.06 (d, 12H, J = 8.8 Hz), 4.03 (t, 8H, J = 7.2 Hz), 3.98 (t, 16H, J = 7.2 Hz), 1.05 (t, 8H, J = 7.2 Hz), 0.92 (t, 16H, J = 7.2 Hz), 0.38 (s, 72H), 0.34 (s, 36H). MALDI-TOF: m/z = 3114.56 (calculated for $C_{172}H_{198}$ $Br_2N_2O_{12}PtZn_2$ $(M+H)^+$ 3111.20).

5,15-Bis[5'-[[15'-triisopropylsilylethynyl-10', 20'-bis(3,5-di(3,3-dimethyl-1-butyloxy)phenyl)porphinato]zinc(II)]ethynyl]-[10,20-bis(2',6'-bis(3,3-dimethyl-1-butyloxy)phenyl)porphinato]platinum(II) (TIPS-EPZnPPtPZnE-TIPS). A 50 mL Schlenk flask equipped with a magnetic stirbar was charged with **BrPZnPPtPZnBr** (80 mg, 0.026 mmol), $Pd(PPh_3)_2Cl_2$ (9.1 mg, 0.013 mmol), and CuI (2.5 mg, 0.013 mmol). A solvent mixture of THF (25 mL), diisopropylamine (2.5 ml) and (triisopropylsilyl)acetylene (59 µL, 0.26 mmol) was degassed via three-pump-thaw cycles, transferred to the reaction flask, and stirred at 60 °C for 16 h. After the reaction endpoint was confirmed by TLC, the reaction mixture was poured into water, extracted with CH_2Cl_2, dried over Na_2SO_4, and evaporated. The residue was purified by column chromatography using 1:1 hexanes:methylene chloride as the eluent. Yield = 67 mg (78%, based on 80 mg of **BrPZnPPtPZnBr**). ^{1}H NMR (400MHz, $CDCl_3$ as 7.26 ppm): δ 10.28 (d, 4H, J = 4.4 Hz), 10.19 (d, 4H, J = 4.8), 9.70 (d, 4H, J = 4.4 Hz), 9.04 (d, 4H, J = 4.4 Hz), 8.92 (t, 8H, J = 4.4 Hz), 7.75 (t, 2H, J = 8.4 Hz), 7.74 (t, 4H, J = 8.4 Hz), 7.06 (d, 4H, J = 8.8 Hz), 7.05 (d, 8H, J = 8.4 Hz), 4.02 (t, 8H, J = 7.2 Hz), 3.98 (t, 16H, J = 7.2 Hz), 1.50-1.44 (m, 42H), 1.04 (t, 8H, J = 7.2 Hz), 0.94 (t, 16H, J = 7.2 Hz), 0.33 (s, 108 H). MALDI-TOF: m/z = 3317.28 (calculated for $C_{194}H_{240}N_{12}O_{12}Si_2PtZn_2$ $(M+H)^+$ 3314.14).

5,15-Bis[5'-[[15'-ethynyl-10', 20'-bis(3,5-di(3,3-dimethyl-1-butyloxy)phenyl)porphinato]zinc(II)]ethynyl]-[10,20-bis(2',6'-bis(3,3-dimethyl-1-butyloxy)phenyl)porphinato]platinum(II) (EPZnPPtPZnE). Tetrabutylammonium fluoride (1M in THF, 37 µL, 0.037 mmol) was added to a solution of **TIPS-EPZnPPtPZnE-TIPS** (50 mg, 0.015 mmol) in THF (20 ml) under argon at 0 °C. The reaction mixture was stirred for 10 min at 0 °C, quenched with water, extracted with CH_2Cl_2, dried over Na_2SO_4, and evaporated. The residue was chromatographed on silica gel using 8:2 hexanes:THF as the eluent. Yield = 43 mg (97%, based on 50 mg of **TIPS-EPZnPPtPZnE-TIPS**). ^{1}H NMR (400MHz, $CDCl_3$ as 7.26 ppm): δ 10.26 (d, 4H, J = 4.4 Hz), 10.17 (d, 4H, J = 4.8), 9.71 (d, 4H, J = 4.4 Hz), 9.03 (d, 4H, J = 4.4 Hz), 8.92 (t, 8H, J = 4.4 Hz), 7.75 (t, 2H, J = 8.4 Hz), 7.73 (t, 4H, J = 8.4 Hz), 7.07 (d, 4H, J = 8.8 Hz), 7.05 (d, 8H, J = 8.4 Hz), 4.07 (s, 2H), 4.00 (t, 8H, J = 7.2 Hz), 3.96 (t, 16H, J = 7.2 Hz), 1.50-1.44 (m, 42H), 1.04 (t, 8H, J = 7.2 Hz), 0.93 (t, 16H, J = 7.2 Hz), 0.32 (s, 108 H). MALDI-TOF: m/z = 3004.52 (calculated for $C_{176}H_{200}N_{12}O_{12}PtZn_2$ $(M+H)^+$ 3001.45).

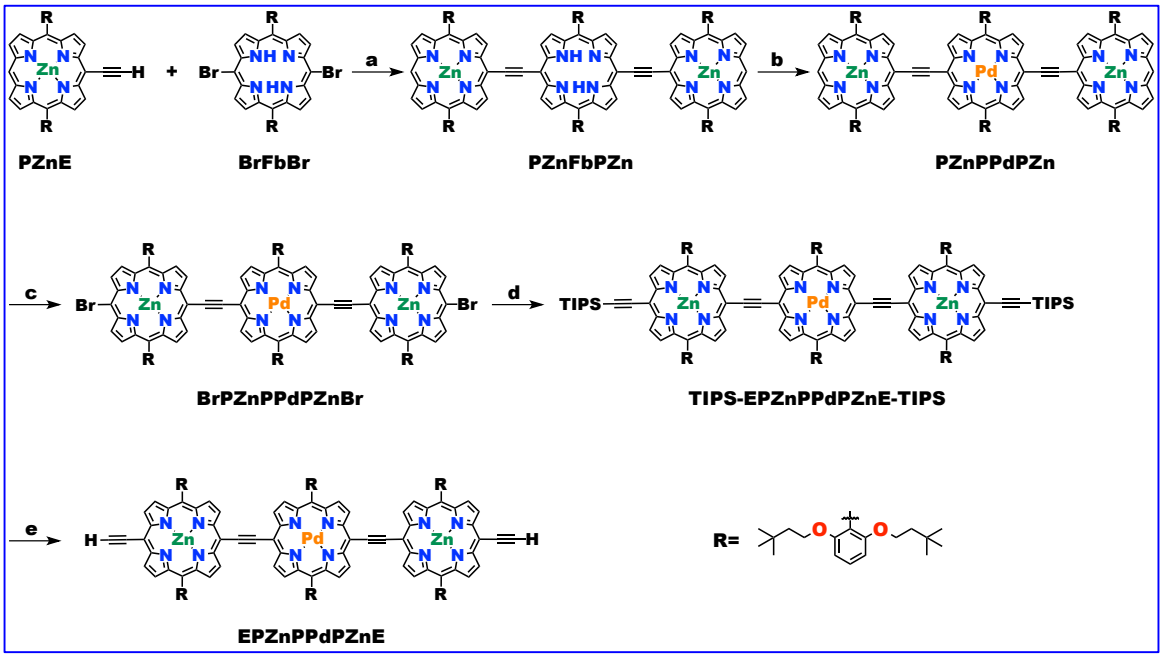

Scheme S5. Synthesis of **EPZnPPdPZnE**. (a) $Pd_2(dba)_3$, $AsPh_3$, THF:*i*-Pr_2NH 9:1 mixture, 50 °C, 12 h, under argon; (b) $Pd(OAc)_2$, benzonitrile, 200 °C, 3 h, microwave reaction; (c) NBS, 0 °C, CH_2Cl_2:pyridine 20:1 mixture, 1.5 h, under argon; (d) (triisopropylsilyl)acetylene, $Pd(PPh_3)_2Cl_2$, CuI, THF:*i*-Pr_2NH 9:1 mixture, 60 °C, 16 h, under argon; (e) TBAF, THF, 0 °C, 10 min, under argon.

5,15-Bis[5'-[[10', 20'-bis(3,5-di(3,3-dimethyl-1-butyloxy)phenyl)porphinato]zinc(II)]ethynyl]-10,20-bis(2',6'-bis(3,3-dimethyl-1-butyloxy)phenyl)porphyrin (PZnFbPZn). A 100 mL Schlenk flask equipped with a magnetic stirbar was charged with **PZnE** (400 mg, 0.42 mmol), **BrFbBr** (170 mg, 0.17 mmol), $Pd_2(dba)_3$ (38 mg, 0.042 mmol), and $AsPh_3$ (51 mg, 0.168 mmol). A solvent mixture of THF (50 mL) and diisopropylamine (5ml) was degassed via five freeze-pump-thaw cycles, transferred to the reaction flask and stirred at 50 °C for 12 h. After the reaction endpoint was confirmed by TLC, the reaction mixture was evaporated to dryness and the residue was sequentially purified by silica column chromatography using 6:4 hexanes:methylene chloride as the eluent, size exclusion column chromatography using THF as the eluent, and another silica column chromatographic step using 1:1 hexanes:methylene chloride as the eluent. Yield = 206 mg (44%, based on 170 mg of **BrFbBr**). ^{1}H NMR (400MHz, $CDCl_3$ as 7.26 ppm): δ 10.42 (d, 4H, J = 4.4 Hz), 10.28 (d, 4H, J = 4.8), 10.10 (s, 2H), 9.28 (d, 4H, J = 4.4 Hz), 9.15 (d, 4H, J = 4.8 Hz), 9.00 (d, 4H, J = 4.4 Hz), 8.98 (d, 4H, J = 4.8 Hz), 7.78 (t, 2H, J = 8.4 Hz), 7.77 (t, 4H, J = 8.4), 7.09 (d, 4H, J = 8.8 Hz), 7.08 (d, 8H, J = 8.4 Hz), 4.04 (t, 8H, J = 7.2 Hz), 3.99 (t, 16H, J = 7.2 Hz), 1.043 (t, 8H, J =

7.2 Hz), 0.93 (t, 16H, J = 7.2 Hz), 0.41 (s, 36H), 0.31 (s, 72H), -1.19 (s, 2H). MALDI-TOF: m/z = 2757.64 (calculated for $C_{172}H_{202}N_{12}O_{12}Zn_2$ $(M+H)^+$ 2760.34).

5,15-Bis[5'-[[10', 20'-bis(3,5-di(3,3-dimethyl-1-butyloxy)phenyl)porphinato]zinc(II)]ethynyl]-[10,20-bis(2',6'-bis(3,3-dimethyl-1-butyloxy)phenyl)porphinato]palladium(II) (PZnPPdPZn). PZnFbPZn (65 mg, 0.024 mmol), palladium acetate (32 mg, 0.144 mmol) and a magnetic stirring bar were brought together into a 10 mL microwave reaction vial that was then sealed and charged with argon. These reagents were dissolved in 6 mL of benzonitrile solvent that was previously purged with argon for 1 h. The reaction vial was stirred at 200 ^oC for 3 h in a microwave irradiation cavity. After the reaction without removing the benzonitrile solvent, the reaction mixture was directly purified by silica column chromatography using 65:35 hexanes:methylene chloride as the eluent; the first brownish green band was collected as the desired product. This reaction was repeated for two additional times in order to obtain material for subsequent synthetic steps. Yield = 134 mg (products from 3 reactions, 65%, based on 195 mg of the **PZnFbPZn** starting material). ^1H NMR (400MHz, $CDCl_3$ as 7.26 ppm): δ 10.39 (d, 4H, J = 4.4 Hz), 10.29 (d, 4H, J = 4.8), 10.11 (s, 2H), 9.28 (d, 4H, J = 4.4 Hz), 9.15 (d, 4H, J = 4.4 Hz), 9.00 (d, 4H, J = 4.4 Hz), 8.97 (d, 4H, J = 4.8 Hz), 7.76 (t, 6H, J = 8.8 Hz), 7.08 (d, 8H, J = 8.4 Hz), 7.07 (d, 4H, J = 8.8 Hz), 4.03 (t, 8H, J = 7.2 Hz), 3.98 (t, 16H, J = 7.2 Hz), 1.04 (t, 8H, J = 7.2 Hz), 0.93 (t, 16H, J = 7.2 Hz), 0.30 (s, 108H). MALDI-TOF: m/z = 2860.52 (calculated for $C_{172}H_{200}N_{12}O_{12}PdZn_2$ $(M+H)^+$ 2864.74).

5,15-Bis[5'-[[15'-bromo-10', 20'-bis(3,5-di(3,3-dimethyl-1-butyloxy)phenyl)porphinato]zinc(II)]ethynyl]-[10,20-bis(2',6'-bis(3,3-dimethyl-1-butyloxy)phenyl)porphinato]palladium(II) (BrPZnPPdPZnBr). In a 250 mL round bottom flask, **PZnPPdPZn** (120 mg, 0.042 mmol) was dissolved in methylene chloride (50 mL) and pyridine (5 mL). The reaction mixture was cooled to 0 °C and a solution of NBS (15 mg, 0.088 mmol) in methylene chloride (50 mL) was added via cannula. The reaction mixture was stirred at 0 °C under argon for 1.5 h and quenched by addition of H_2O (100 mL). The organic layer was separated and dried with anhydrous Na_2SO_4. After evaporation of the solvent, the residue was purified by column chromatography using 6:4 hexanes:methylene chloride as the eluent. Yield = 79 mg (62 %, based on 120 mg of the **PZnPPdPZn** starting material). ^1H NMR (400MHz, $CDCl_3$ as 7.26 ppm): δ 10.29 (d, 4H, J = 4.8 Hz), 10.25 (d, 4H, J = 4.8), 9.63 (d, 4H, J = 4.8 Hz),

9.03 (d, 4H, J = 4.8 Hz), 8.96 (d, 4H, J = 4.8 Hz), 8.88 (d, 4H, J = 4.8 Hz), 7.76 (t, 2H, J = 8.4 Hz), 7.75 (t, 4H, J = 8.4 Hz), 7.07 (d, 4H, J = 8.8 Hz), 7.06 (d, 8H, J = 8.8 Hz), 4.02 (t, 8H, J = 7.2 Hz), 3.98 (t, 16H, J = 7.2 Hz), 1.03 (t, 8H, J = 7.2 Hz), 0.92 (t, 16H, J = 7.2 Hz), 0.38 (s, 72H) , 0.30 (s, 36H). MALDI-TOF: m/z = 3018.26 (calculated for $C_{172}H_{198}$ $Br_2N_2O_{12}PdZn_2$ $(M+H)^+$ 3022.54).

5,15-Bis[5'-[[15'-triisopropylsilylethynyl-10', 20'-bis(3,5-di(3,3-dimethyl-1-butyloxy)phenyl)porphinato]zinc(II)]ethynyl]-[10,20-bis(2',6'-bis(3,3-dimethyl-1-butyloxy)phenyl)porphinato]palladium(II) (TIPS-EPZnPPdPZnE-TIPS). A 50 mL Schlenk flask equipped with a magnetic stirbar was charged with **BrPZnPPdPZnBr** (70 mg, 0.023 mmol), $Pd(PPh_3)_2Cl_2$ (8.4 mg, 0.012 mmol), and CuI (2.3 mg, 0.012 mmol). A solvent mixture of THF (20 mL), diisopropylamine (2 ml) and (triisopropylsilyl)acetylene (52 µL, 0.23 mmol) was degassed via three-pump-thaw cycles, transferred to the reaction flask and stirred at 60 °C for 16 h. After the reaction endpoint was confirmed by TLC, the reaction mixture was poured into water, extracted with CH_2Cl_2, dried over Na_2SO_4, and evaporated. The residue was purified by column chromatography using 1:1 hexanes: methylene chloride as the eluent. Yield = 54 mg (73%, based on 70 mg of **BrPZnPPdPZnBr**). ^{1}H NMR (400MHz, $CDCl_3$ as 7.26 ppm): δ 10.30 (d, 4H, J = 4.4 Hz), 10.24 (d, 4H, J = 4.8), 9.70 (d, 4H, J = 4.4 Hz), 9.04 (d, 4H, J = 4.4 Hz), 8.97 (d, 4H, J = 4.8 Hz), 8.91 (d, 4H, J = 4.4 Hz), 7.75 (t, 2H, J = 8.4 Hz), 7.74 (t, 4H, J = 8.4 Hz), 7.06 (d, 4H, J = 8.4 Hz), 7.05 (d, 8H, J = 8.8 Hz), 4.02 (t, 8H, J = 7.2 Hz), 3.98 (t, 16H, J = 7.2 Hz), 1.50-1.45 (m, 42H), 1.01 (t, 8H, J = 7.2 Hz), 0.90 (t, 16H, J = 7.2 Hz), 0.33 (s, 72H) , 0.29 (s, 36H). MALDI-TOF: m/z = 3221.94 (calculated for $C_{194}H_{240}N_2O_{12}Si_2PdZn_2$ $(M+H)^+$ 3225.48).

5,15-Bis[5'-[[15'-ethynyl-10', 20'-bis(3,5-di(3,3-dimethyl-1-butyloxy)phenyl)porphinato]zinc(II)]ethynyl]-[10,20-bis(2',6'-bis(3,3-dimethyl-1-butyloxy)phenyl)porphinato]palladium(II) (EPZnPPdPZnE). Tetrabutylammonium fluoride (1 M in THF, 43 µL, 0.043 mmol) was added to a solution of **TIPS-EPZnPPdPZnE-TIPS** (54 mg, 0.017 mmol) in THF (30 ml) under argon at 0 °C. The reaction mixture was stirred for 10 min at 0 °C, quenched with water, extracted with CH_2Cl_2, dried over Na_2SO_4, and evaporated. The residue was chromatographed on silica gel using 8:2 hexanes:THF as the eluent. Yield = 46 mg (95%, based on 54 mg of **TIPS-EPZnPPdPZnE-TIPS**). ^{1}H NMR (400MHz, $CDCl_3$ as 7.26 ppm): δ 10.29 (d, 4H, J = 4.4 Hz), 10.22 (d, 4H, J = 4.8), 9.69 (d, 4H, J = 4.4 Hz), 9.03 (d, 4H, J

= 4.4 Hz), 8.96 (d, 4H, J = 4.8 Hz), 8.92 (d, 4H, J = 4.4 Hz), 7.76 (t, 2H, J = 8.4 Hz), 7.75 (t, 4H, J = 8.4 Hz), 7.06 (d, 4H, J = 8.4 Hz), 7.05 (d, 8H, J = 8.8 Hz), 4.08 (s, 2H), 4.01 (t, 8H, J = 7.2 Hz), 3.97 (t, 16H, J = 7.2 Hz), 1.50-1.45 (m, 42H), 1.01 (t, 8H, J = 7.2 Hz), 0.91 (t, 16H, J = 7.2 Hz), 0.34 (s, 72H) , 0.30 (s, 36H). MALDI-TOF: m/z = 2908.35 (calculated for $C_{194}H_{240}N_2O_{12}Si_2PdZn_2$ $(M+H)^+$ 2912.79).

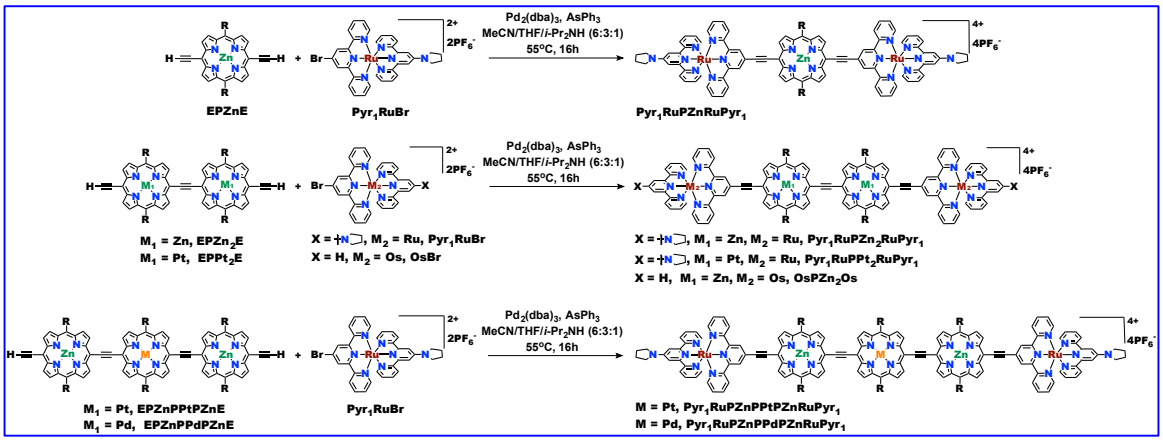

Scheme S6. Schematic summary for the syntheses of **$Pyr_1RuPZnRuPyr_1$, $Pyr_1RuPZn_2RuPyr_1$, $OsPZn_2Os$, $Pyr_1RuPPt_2RuPyr_1$, $Pyr_1RuPZnPPtPZnRuPyr_1$**, and **$Pyr_1RuPZnPPdPZnRuPyr_1$.**

General Procedure for the Preparation of $Pyr_1RuPZnRuPyr_1$, $Pyr_1RuPZn_2RuPyr_1$, and $OsPZn_2Os$. Bis(*meso*-ethynyl) ethyne-bridged oligo(porphinato)zinc(II) derivatives (**EPZnE**, **$EPZn_2E$**) and bis(terpyridyl)metal(II) complexes (**Pyr_1RuBr**, **OsBr**) were placed in a Schlenk flask equipped with a magnetic stir bar. $Pd_2(dba)_3$ (0.3 eq., based on the (porphinato)zinc synthon) and $AsPh_3$ (2 eq., based on the (porphinato)zinc synthon) were added under nitrogen atmosphere. A solvent mixture of 6:3:1 HPLC grade MeCN:THF:triethylamine was degassed by a small stream of dry argon for approximately 2 h. Enough of this solvent mixture was added to the reaction vessel via cannula to completely dissolve all reactants, and the resulting solution was heated to 60 °C for 8 h. Consumption of all the starting materials was confirmed by thin layer chromatography (90:9:1 MeCN:H_2O:saturated aq. KNO_3 as eluent). The solution was then cooled to room temperature and evaporated. The crude product was purified by column chromatography using 90:9:1 MeCN:H_2O:sat. aq. KNO_3 as eluent for **$Pyr_1RuPZnRuPyr_1$, $Pyr_1RuPZn_2RuPyr_1$, $Pyr_1RuPPt_2RuPyr_1$,** and **$OsPZn_2Os$**, whereas for **$Pyr_1RuPZnPPdPZnRuPyr_1$** and **$Pyr_1RuPZnPPtPZnRuPyr_1$**, 70:20:9:1 MeCN:THF:H_2O:sat.

aq. KNO_3 was employed as the eluent; the respective products eluted as the second band, following a first, small quantity of homocoupled butadiyne-bridged side-product. The product fractions was concentrated, but not to dryness. Excess ammonium hexafluorophosphate was added, followed by enough water to cause the precipitation of a dark brown-green solid, which was isolated by filtration, and washed successively with water and diethyl ether. The products were then further purified through size exclusion column chromatography (Bio-beads SX-1 medium) using 1:1 acetone:THF as the eluent, followed by a short silica gel column chromatographic step using the corresponding solvent mixture as eluent (*vide supra*). Additional column chromatography was performed if the level of purity was unsatisfactory as assessed by NMR spectroscopy. Counterion metathesis was then exploited again to provide the corresponding bis(hexafluorophosphate) salts as the final products.

Bisruthenium(II) [(5,15-bis(4'-ethynyl-(2,2';6',2''-terpyridinyl))-10,20-bis(2',6'-bis(3,3-dimethyl-1-butyloxy)phenyl)porphinato)zinc(II)] [4'-pyrrolidin-1-yl-2,2';6',2''-terpyridine] tetrakis(hexafluorophosphate) (Pyr$_1$RuPZnRuPyr$_1$). Reagents: **EPZnE** (68 mg, 0.070 mmol), **Pyr$_1$RuBr** (176 mg, 0.0175 mmol), $Pd_2(dba)_3$ (19.2 mg, 0.021 mmol), and $AsPh_3$ (43 mg, 0.14 mmol). Reaction solvent: 40 mL of 6:3:1 MeCN:THF:triethylamine. Isolated yield = 160 mg of **Pyr$_1$RuPZnRuPyr$_1$** (81%, based on 68 mg of **EPZnE**). ^{1}HNMR (400MHz, CD_3CN as 1.93 ppm): δ 9.77 (d, 4H, J = 4.4 Hz), 9.14 (s, 4H), 8.75 (d, 4H, J = 4.4 Hz), 8.58 (d, 4H, J = 8.0 Hz), 8.30 (d, 4H, J = 8.0 Hz), 7.84 (t, 4H, J = 7.0 Hz), 7.70-7.63 (m, 10H), 7.39 (d, 4H, J = 5.0 Hz), 7.21 (d, 4H, J = 5.0 Hz), 7.12 (t, 4H, J = 6.0 Hz), 6.99 (d, 4H, J = 8.5 Hz), 6.92 (t, 4H, J =6.0 Hz), 3.83 (t, 8H, J = 7.0 Hz), 3.63 (s, 8H), 2.07 (s, 8H), 0.66 (t, 8H, J = 7.0 Hz), 0.03 (s, 36H). MALDI-TOF: m/z = 2675.37 (calculated for $C_{128}H_{122}F_{18}N_{18}O_4P_3Ru_2Zn$ $(M\text{-}PF_6)^+$ 2678.92).

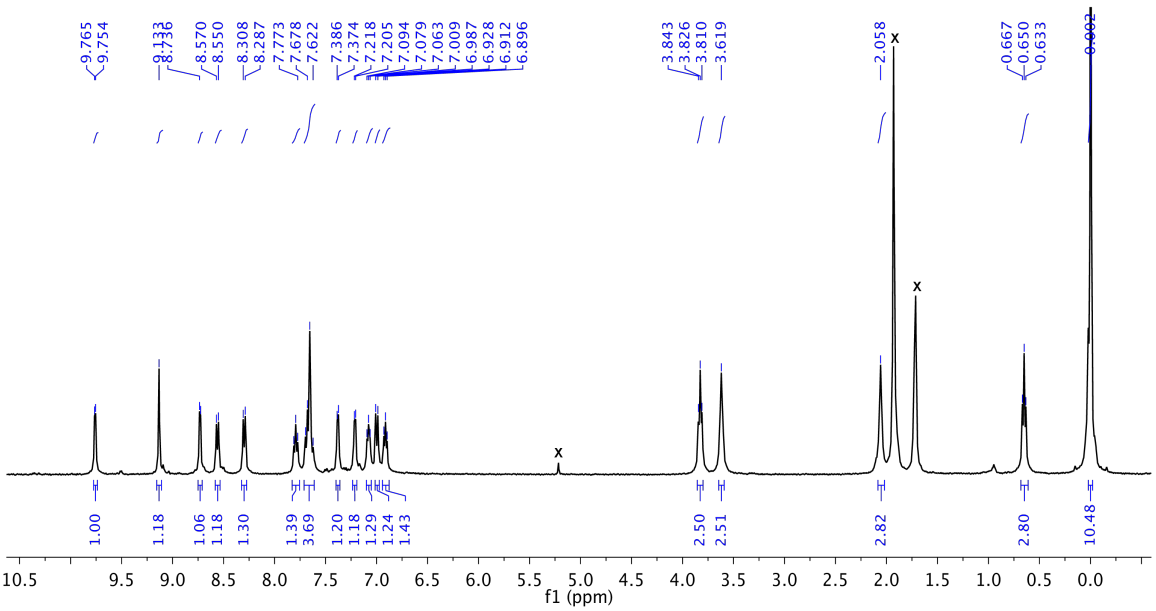

Figure S1. ^{1}H NMR spectrum of **Pyr$_1$RuPZnRuPyr$_1$** in CD_3CN solvent, residual solvent (CH_2Cl_2, MeCN, and THF) peaks are marked with "X".

Bisruthenium(II) [1,2-bis[(5-(4'-ethynyl-(2,2';6',2''-terpyridinyl))-10,20-bis(2',6'-bis(3,3-dimethyl-1-butyloxy)phenyl)porphinato)zinc(II)]ethyne] [4'-pyrrolidin-1-yl-2,2';6',2''-terpyridine] tetrakis(hexafluorophosphate) (Pyr$_1$RuPZn$_2$RuPyr$_1$). Reagents: **EPZn$_2$E** (100 mg, 0.052 mmol), **Pyr$_1$RuBr** (115 mg, 0.114 mmol), $Pd_2(dba)_3$ (14.3 mg, 0.0156 mmol), and $AsPh_3$ (32 mg, 0.104 mmol). Reaction solvent: 40 mL of 6:3:1 MeCN:THF:triethylamine. Isolated yield = 125 mg (63%, based on 100 mg of **EPZn$_2$E**). ^{1}HNMR (400MHz, CD_3CN as 1.93 ppm): δ 9.97 (d, 4H, J = 4.4 Hz), 9.72 (d, 4H, J = 4.4 Hz), 9.09 (s, 4H), 8.71 (d, 4H, J = 4.8 Hz), 8.68 (d, 4H, J = 4.8 Hz), 8.49 (d, 4H, J = 8.0 Hz), 8.21 (d, 4H, J = 8.0 Hz), 7.66 (t, 4H, J = 7.6 Hz), 7.61 (t, 4H, J = 8.4 Hz), 7.57 (s, 4H), 7.49 (t, 4H, J = 7.6 Hz), 7.32 (d, 4H, J = 4.8 Hz), 7.13 (d, 4H, J = 5.6 Hz), 6.99-6.94 (m, 12H), 6.72 (t, 4H, J = 6.4 Hz), 3.81 (t, 16H, J = 7.0 Hz), 3.46 (s, 8H), *~1.90 (s, 8H)* (note that this peak is not observed in the NMR spectrum below as it is completely overlapped by the residual MeCN solvent peak), 0.65 (t, 16H, J = 7.0 Hz), 0.01 (s, 72H). MALDI-TOF: m/z = 3624.87 (calculated for $C_{186}H_{188}F_{18}N_{22}O_8P_3Ru_2Zn_2$ $(M\text{-}PF_6)^+$ 3627.49).

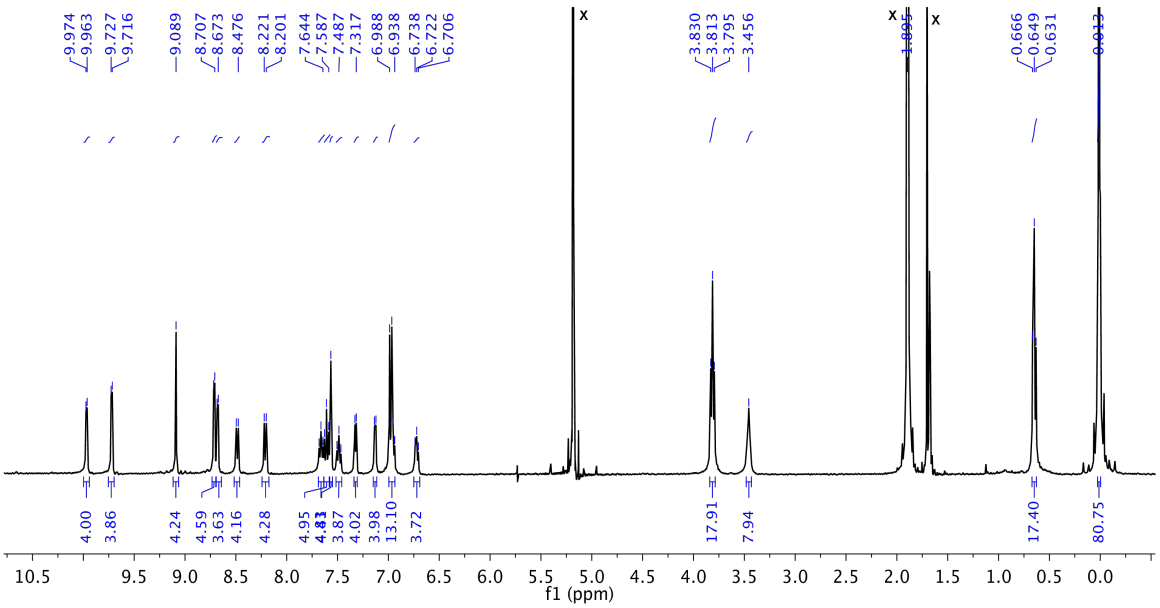

Figure S2. ^{1}H NMR spectrum of **Pyr$_1$RuPZn$_2$RuPyr$_1$** in CD_3CN solvent, residual solvent (CH_2Cl_2, MeCN, and THF) peaks are marked with "X".

Bisosmium(II) [1,2-bis[(5-(4'-ethynyl-(2,2';6',2''-terpyridinyl))-10,20-bis(2',6'-bis(3,3-dimethyl-1-butyloxy)phenyl)porphinato)zinc(II)]ethyne] [2,2';6',2''-terpyridine] tetrakis(hexafluorophosphate) (OsPZn$_2$Os). Reagent: **EPZn$_2$E** (46 mg, 0.0238 mmol), **OsBr** (61.5 mg, 0.06 mmol), $Pd_2(dba)_3$ (6.6 mg, 0.0072 mmol), and $AsPh_3$ (14.7 mg, 0.048 mmol). Reaction solvent: 25 mL of 6:3:1 MeCN:THF:triethylamine as outlined in the above procedure. Yield = 75 mg (79% yield based on 46 mg of **EPZn$_2$E**). ^{1}HNMR (400MHz, CD_3CN as 1.93 ppm): δ 10.02 (d, 4H, J = 4.4 Hz), 9.76 (d, 4H, J = 4.4 Hz), 9.18 (s, 4H), 8.76 (d, 4H, J = 7.0 Hz), 8.74 (d, 4H, J = 7.0 Hz), 8.58 (d, 4H, J = 8.4 Hz), 8.52 (d, 4H, J = 8.4 Hz), 8.27 (d, 4H, J = 8.4 Hz), 7.75 (t, 2H, J = 8.4 Hz), 7.63 (t, 4H, J = 8.8 Hz), 7.58 (t, 4H, J = 7.8 Hz), 7.52 (t, 4H, J = 7.8 Hz), 7.19 (d, 4H, J = 6.0 Hz), 7.08 (d, 4H, J = 5.6 Hz), 7.01 (d, 8H, J = 8.8 Hz), 6.87 (q, 8H, J = 6.8 Hz), 3.85 (t, 16H, J = 7.0), 0.69 (t, 16H, J = 7.0 Hz), 0.04 (s, 72H). MALDI-TOF: m/z = 3665.53 (calculated for $C_{178}H_{174}F_{18}N_{20}O_8P_3Os_2Zn_2$ $(M\text{-}PF_6)^+$ 3667.49).

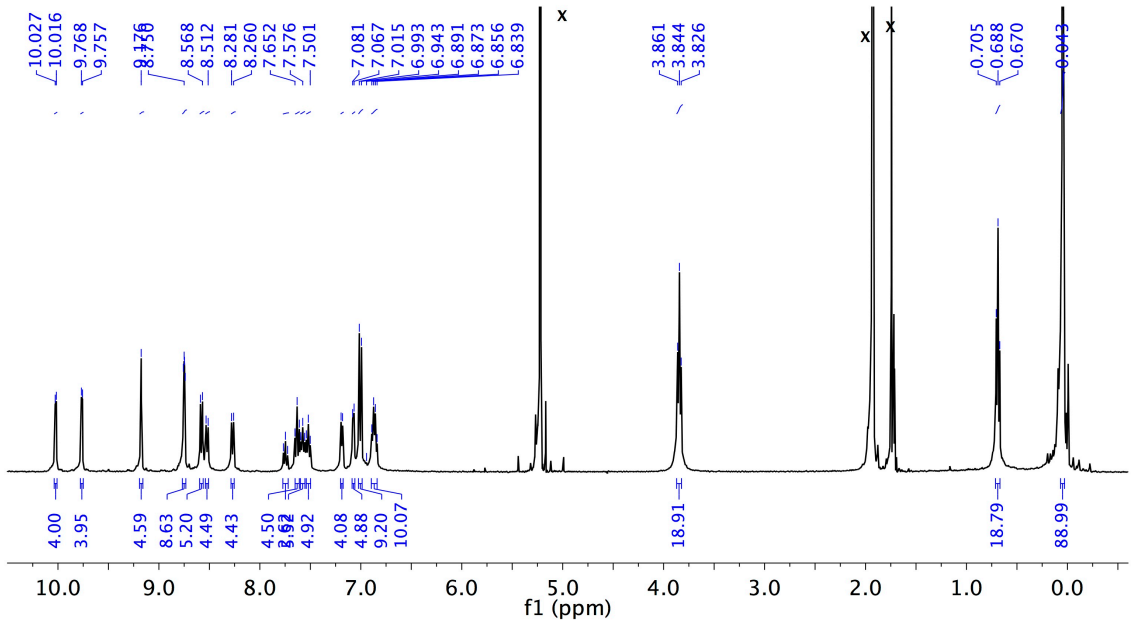

Figure S3. ^{1}H NMR spectrum of **OsPZn$_2$Os** in CD_3CN solvent, residual solvent (CH_2Cl_2, MeCN, and THF) peaks are marked with "X".

Bisruthenium(II) [1,2-bis[(5-(4'-ethynyl-(2,2';6',2''-terpyridinyl))-10,20-bis(2',6'-bis(3,3-dimethyl-1-butyloxy)phenyl)porphinato)platinum(II)]ethyne] [4'-pyrrolidin-1-yl-2,2';6',2''-terpyridine] tetrakis(hexafluorophosphate) (Pyr$_1$RuPPt$_2$RuPyr$_1$). Reagents: **EPPt$_2$E** (35 mg, 0.016 mmol), **Pyr$_1$RuBr** (40 mg, 0.04 mmol), $Pd_2(dba)_3$ (8.8 mg, 0.0096 mmol), and $AsPh_3$ (15 mg, 0.048 mmol). Reaction solvent: 20 mL of 6:3:1 MeCN:THF:triethylamine. Isolated yield = 38 mg (59%, based on 35 mg of **EPZn$_2$E**). ^{1}HNMR (400MHz, CD_3CN as 1.93 ppm): δ 9.88 (d, 4H, J = 4.8 Hz), 9.68 (d, 4H, J = 5.2 Hz), 9.10 (s, 4H), 8.68 (d, 4H, J = 5.2 Hz), 8.66 (d, 4H, J = 4.8 Hz), 8.50 (d, 4H, J = 8.0 Hz), 8.24 (d, 4H, J = 8.4 Hz), 7.74 (t, 4H, J = 7.6 Hz), 7.60 (s, 4H), 7.59 (t, 4H, J = 7.6 Hz), 7.53 (t, 4H, J = 8.4 Hz), 7.33 (d, 4H, J = 5.2 Hz), 7.13 (d, 4H, J = 5.6 Hz), 7.03 (t, 4H, J = 6.4 Hz), 6.88 (d, 8H, J = 8.4 Hz), 6.81 (t, 4H, J = 6.4 Hz), 3.76 (t, 16H, J = 6.4 Hz), 3.56 (t, 8H, J = 6.4 Hz), 2.00 (t, 8H, J = 6.4 Hz), 0.67 (t, 16H, J = 6.8 Hz), -0.141 (s, 72H). MALDI-TOF: m/z = 3889.14 (calculated for $C_{186}H_{188}F_{18}N_{22}O_8P_3Pt_2Ru_2$ $(M-PF_6)^+$ 3886.90).

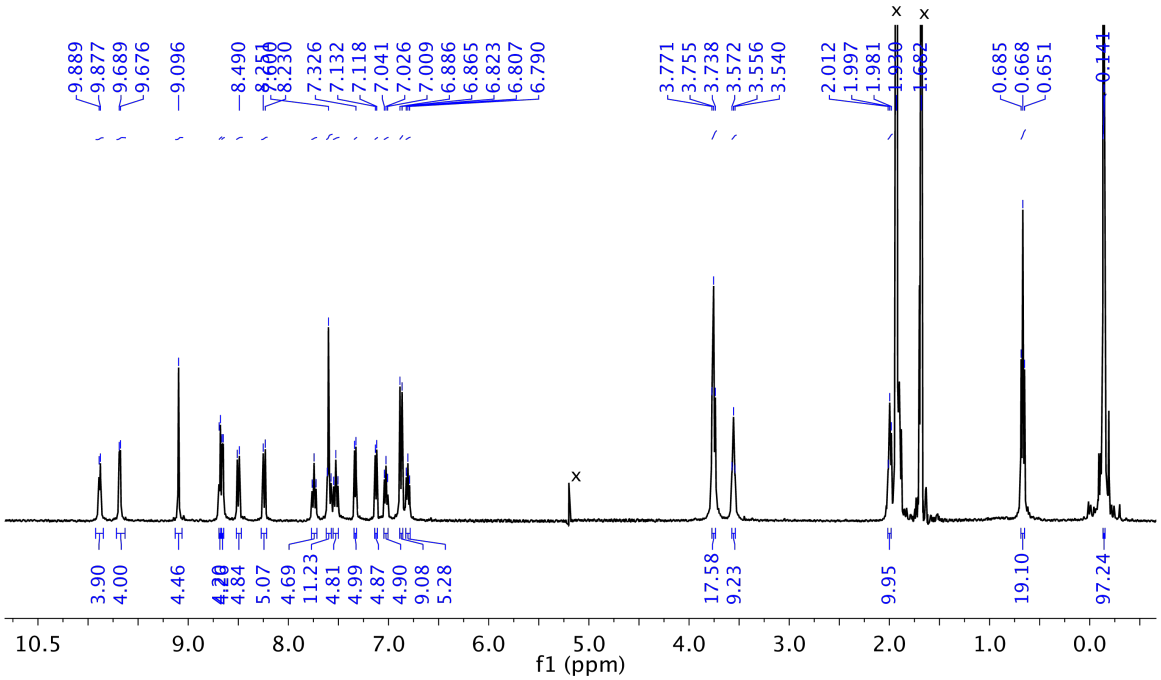

Figure S4. ^{1}H NMR spectrum of **Pyr$_1$RuPPt$_2$RuPyr$_1$** in CD_3CN solvent, residual solvent (CH_2Cl_2, MeCN, and THF) peaks are marked with "X".

Bisruthenium(II) [5,15-bis[5'-ethynyl-[15'-(4'-ethynyl-(2,2';6',2''-terpyridinyl))-10', 20'-bis(3,5-di(3,3-dimethyl-1-butyloxy)phenyl)porphinato]zinc(II)]-[10,20-bis(2',6'-bis(3,3-dimethyl-1-butyloxy)phenyl)porphinato]platinum(II)] [4'-pyrrolidin-1-yl-2,2';6',2''-terpyridine] tetrakis(hexafluorophosphate) (Pyr$_1$RuPZnPPtPZnRuPyr$_1$). Reagents: **EPZnPtPZnE** (30 mg, 0.010 mmol), **Pyr$_1$RuBr** (26 mg, 0.025 mmol), $Pd_2(dba)_3$ (5.5 mg, 0.006 mmol), and $AsPh_3$ (9.2 mg, 0.048 mmol). Reaction solvent: 15 mL of 6:3:1 MeCN:THF:triethylamine. Isolated yield = 30 mg (63%, based on 30 mg of **EPZnPPtPZnE**). ^{1}HNMR (400MHz, CD_3CN as 1.93 ppm): δ 9.94 (d, 4H, J = 4.4 Hz), 9.91 (d, 4H, J = 4.4 Hz), 9.76 (d, 4H, J = 4.4 Hz), 9.11 (s, 4H), 8.74 (d, 4H, J = 4.4 Hz), 8.69 (d, 4H, J = 4.4 Hz), 8.62 (d, 4H, J = 4.8 Hz), 8.51 (d, 4H, J = 8.0 Hz), 8.21 (d, 4H, J = 8.0 Hz), 7.70 (t, 4H, J = 7.6 Hz), 7.58 (t, 4H, J = 8.8 Hz), 7.56 (s, 4H), 7.49 (t, 2H, J = 8.8 Hz), 7.44 (t, 4H, J = 7.6 Hz), 7.36 (d, 4H, J = 5.6 Hz), 7.12 (d, 4H, J = 5.6 Hz), 6.98 (t, 4H, J = 6.4 Hz), 6.94 (d, 8H, J = 8.8 Hz), 6.82 (d, 4H, J = 8.8 Hz), 6.67 (t, 4H, J = 6.4 Hz), 3.77 (t, 16H, J = 6.8 Hz), 3.70 (t, 8H, J = 6.4 Hz), 3.40 (s, 8H), 1.82 (s, 8H), 0.67-0.60 (m, 24H), 0.01 (s, 72H), -0.11 (s, 36). MALDI-TOF: m/z = 4701.82 (calculated for $C_{244}H_{254}F_{18}N_{26}O_{12}P_3PtRu_2Zn_2$ $(M\text{-}PF_6)^+$ 4705.76).

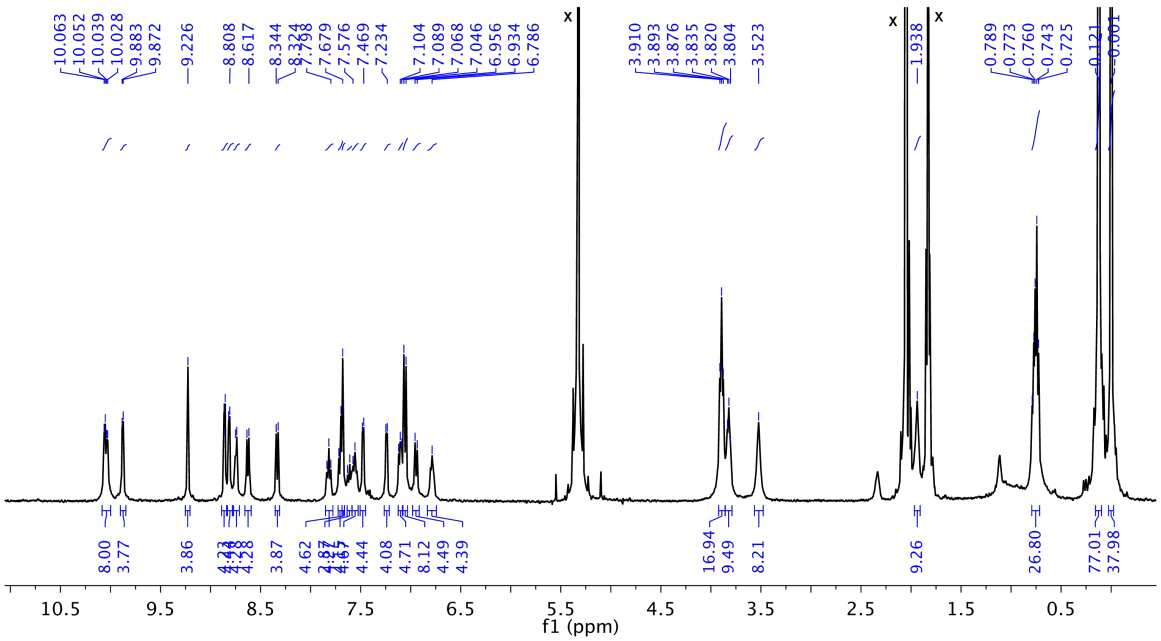

Figure S5. ^{1}H NMR spectrum of **Pyr$_1$RuPZnPPtPZnRuPyr$_1$** in CD_3CN solvent, residual solvent (CH_2Cl_2, MeCN, and THF) peaks are marked with "X".

Bisruthenium(II) [5,15-bis[5'-ethynyl-[15'-(4'-ethynyl-(2,2';6',2''-terpyridinyl))-10', 20'-bis(3,5-di(3,3-dimethyl-1-butyloxy)phenyl)porphinato]zinc(II)]-[10,20-bis(2',6'-bis(3,3-dimethyl-1-butyloxy)phenyl)porphinato]palladium(II)] [4'-pyrrolidin-1-yl-2,2';6',2''-terpyridine] tetrakis(hexafluorophosphate) (Pyr$_1$RuPZnPPdPZnRuPyr$_1$). Reagents: **EPZnPdPZnE** (32 mg, 0.011 mmol), **Pyr$_1$RuBr** (28 mg, 0.027 mmol), $Pd_2(dba)_3$ (6.0 mg, 0.0066 mmol), and $AsPh_3$ (10.1 mg, 0.033 mmol). Reaction solvent: 15 mL of 6:3:1 MeCN:THF:triethylamine. Isolated yield = 28 mg (54%, based on 32 mg of **EPZnPPdPZnE**). ^{1}HNMR (400MHz, TMS as 0 ppm): δ 10.25 (d, 4H, J = 4.4 Hz), 10.23 (d, 4H, J = 4.4 Hz), 9.36 (d, 4H, J = 4.4 Hz), 8.98-8.94 (m, 12H), 8.78 (d, 4H, J = 8.0 Hz), 8.49 (d, 4H, J = 8.4 Hz), 8.02 (t, 4H, J = 7.2 Hz), 7.87-7.77 (m, 14H), 7.60 (d, 4H, J = 4.4 Hz), 7.41 (d, 4H, J = 4.4 Hz), 7.29 (t, 4H, J = 4.8 Hz), 7.22-7.16 (m, 12H), 7.05 (t, 4H, J = 4.8 Hz), 4.05 (t, 24H, J = 6.4 Hz), 3.76 (s, 8H), *~1.90 (s, 8H)* (note that this peak is not observed in the NMR spectrum below as it is completely overlapped by the residual MeCN solvent peak), 0.90 (t, 24H, J = 6.4 Hz), 0.27 (s, 72H), 0.17 (s, 36). MALDI-TOF: m/z = 4619.68 (calculated for $C_{244}H_{254}F_{18}N_{26}O_{12}P_3PdRu_2Zn_2$ $(M\text{-}PF_6)^+$ 4617.10).

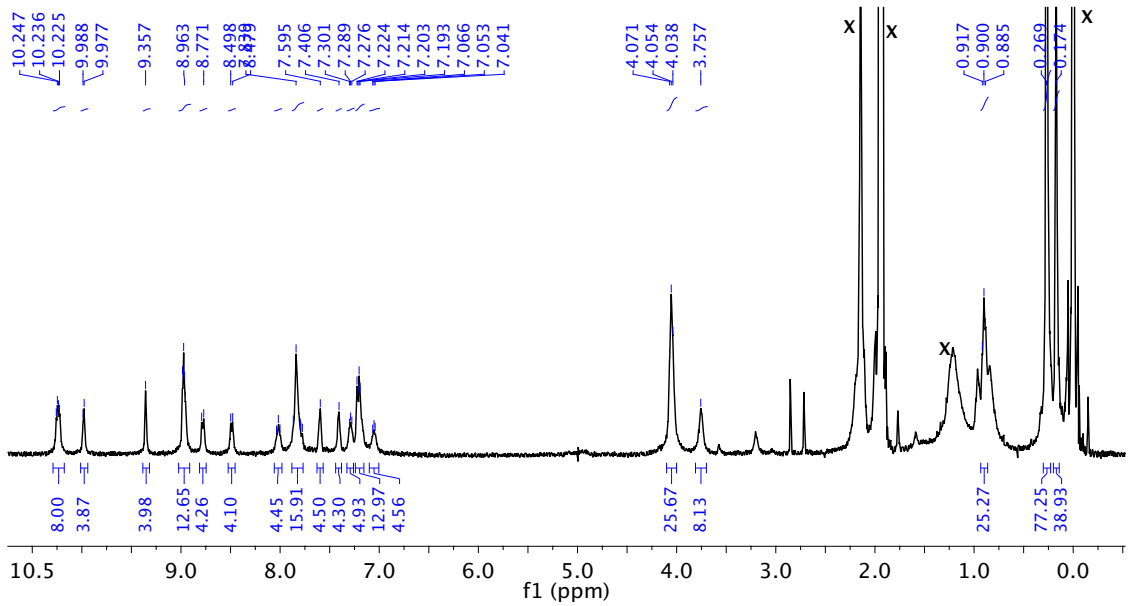

Figure S6. ^{1}H NMR spectrum of **Pyr$_1$RuPZnPPdPZnRuPyr$_1$** in CD_3CN solvent, residual solvent (MeCN, THF, hexanes, and TMS) peaks are marked with "X".

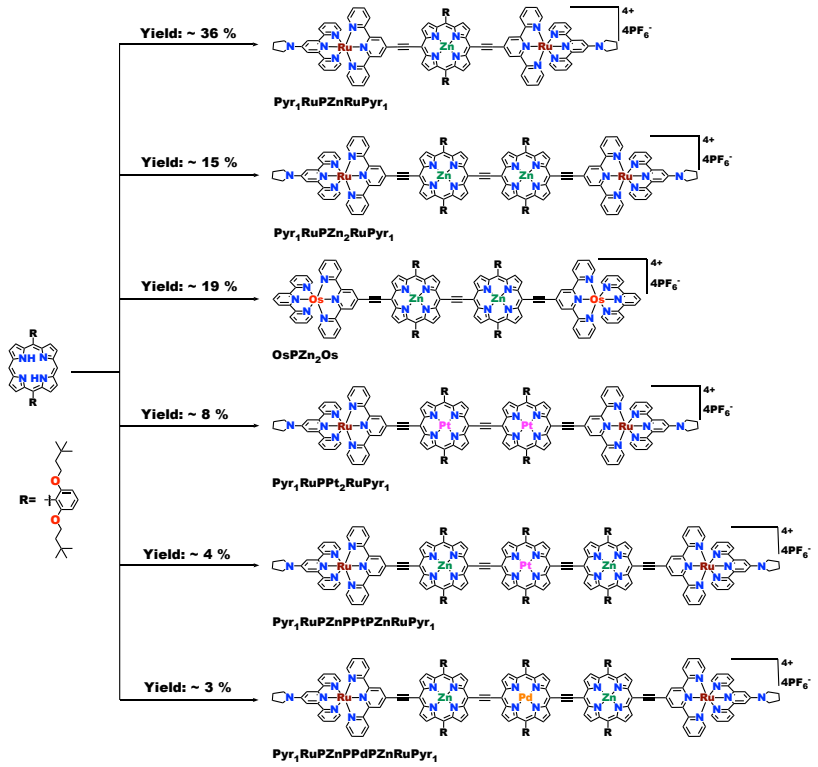

Scheme S7. Schematic summary of the overall reaction yields for **Pyr$_1$RuPZnRuPyr$_1$, Pyr$_1$RuPZn$_2$RuPyr$_1$, OsPZn$_2$Os, Pyr$_1$RuPPt$_2$RuPyr$_1$, Pyr$_1$RuPZnPPtPZnRuPyr$_1$**, and **Pyr$_1$RuPZnPPdPZnRuPyr$_1$**, based on the **10,20-bis(2',6'-bis(3,3-dimethyl-1-butyloxy)phenyl)porphyrin** starting material.

3. Steady-State Emission Spectra of M-PM and $(PM)_n$ Supermolecular Species

3.1 Experimental conditions. The emission spectroscopy of all **M-(PM')$_n$-M** and **(PM)$_n$** supermolecular species were investigated at ambient temperature under both deoxygenated and oxygenated conditions. Deoxygenation was achieved through three freeze-pump-thaw-degas cycles; corresponding oxygenated solutions were prepared by purging with air for 30 min. Multi-wavelength excitation was performed on all these chromophores to demonstrate that no excitation wavelength dependence existed in the experiments, and the optical density under all these excitation wavelengths was ≤ 0.1. Excitation spectra confirmed the authenticity of the emission peaks. Note that the emission spectra are provided separately in two wavelength regimes: starting point (normally between 650 and 700 nm) – 1000 nm and 950 nm – 1350 nm, due to the fact that detection was provided using a combination of a vis-NIR PMT (detection range: 200-1010 nm) and a NIR-PMT (detection range: 950-1700 nm).

3.2 Proof of Concept Study – Photophysical Properties of PZnPPtPZn. As shown in Figure S12, **PZnPPtPZn** demonstrates a Q_x transition maximum absorption centered at 708 nm that is significantly red-shifted ($\Delta\lambda$ = 72 nm) when compared to the previous established **PPt$_3$** benchmark.[4] The emission and nanosecond transient absorption spectroscopic experiments chronicled in Figures S12 and S24 demonstrate that **PZnPPtPZn** i) possesses a low-lying triplet excited state as confirmed by the emission peak centered at 1083 nm that vanishes under experimental conditions that give rise to molecular oxygen triplet sensitization and subsequent singlet oxygen radiative deactivation (λ_{em} = 1270 nm) and ii) a triplet excited state lifetime of 3.96 μs. The triplet excited state dynamics of **PZnPPtPZn** suggest the promise of the ruthenium-derived hybrid superstructure **Pyr$_1$RuPZnPPtPZnRuPyr$_1$**, for which a near-unity *ISC* with μs scale triplet excited state lifetime and a strong NIR absorptivity are anticipated.

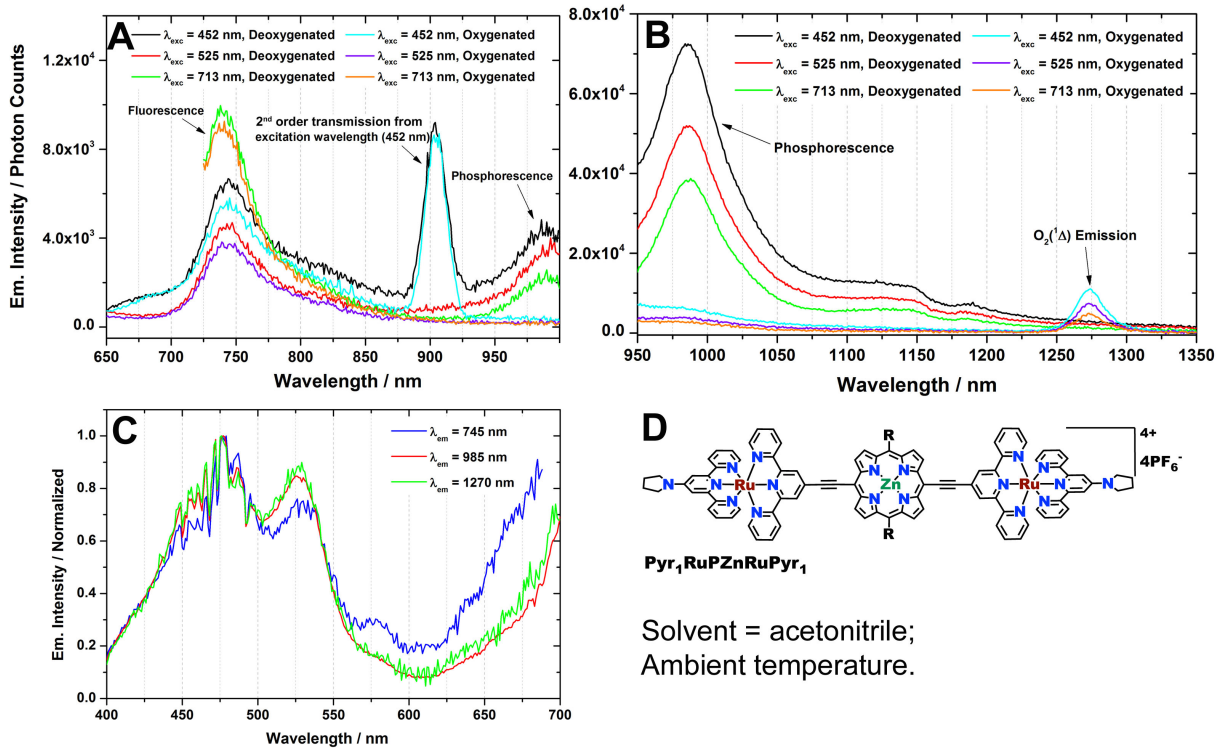

Figure S7. (A) and (B): **Pyr$_1$RuPZnRuPyr$_1$** emission spectra taken under deoxygenated and oxygenated conditions, with peak assignments marked in the spectra; note that while proper long-pass filters have been applied, 2nd order transmission is observed when exciting at 452 nm (this spectroscopic feature is also manifest in some of the emission spectra that follow below). (C) Excitation scanning spectra for **Pyr$_1$RuPZnRuPyr$_1$**; the emission peaks centered at 745 nm, 985 nm and 1270 nm are monitored. (D) Chemical structure of **Pyr$_1$RuPZnRuPyr$_1$**, and general experimental conditions; R group denotes 2'6'-bis(3,3-dimethyl-1butyloxy)phenyl.

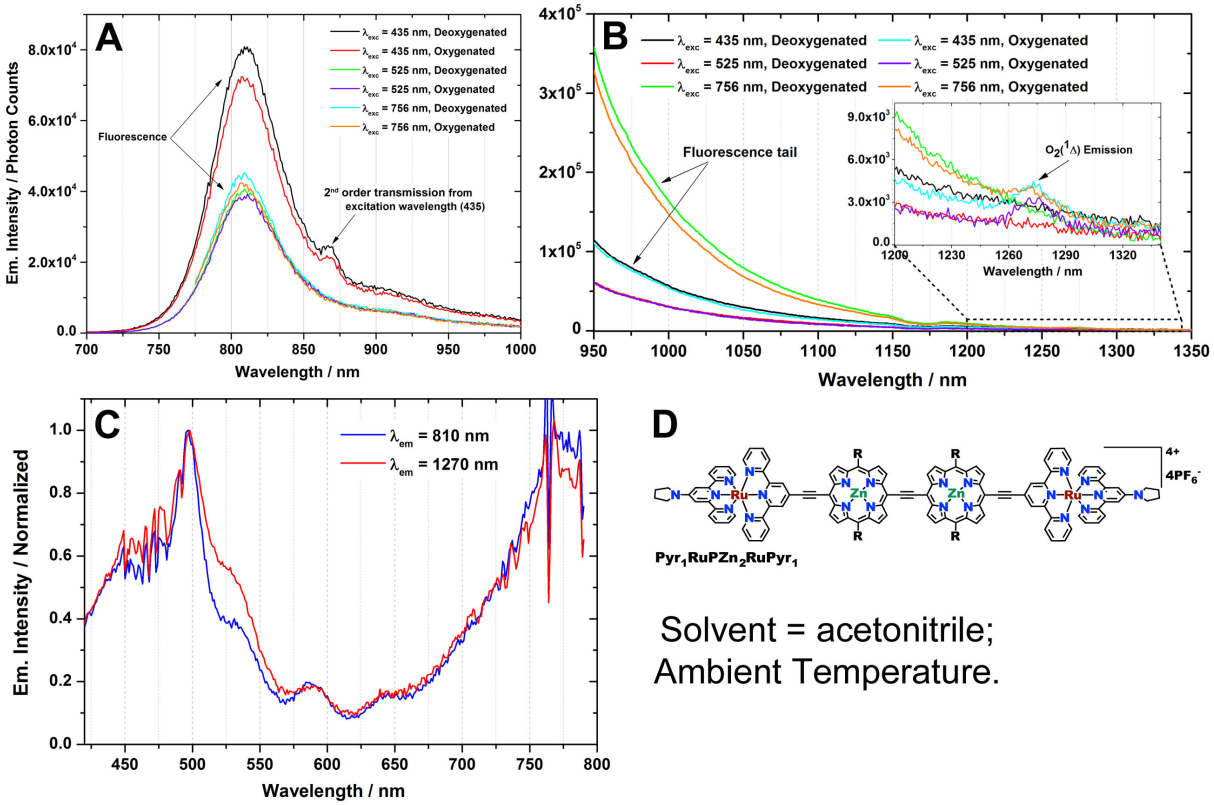

Figure S8. (A) and (B): **Pyr$_1$RuPZn$_2$RuPyr$_1$** emission spectra taken under deoxygenated and oxygenated conditions, with peak assignments marked in the spectra; the panel B inset highlights the spectral window from 1200 nm to 1340 nm (containing *O_2 emission peak). (C) Excitation scanning spectra for **Pyr$_1$RuPZn$_2$RuPyr$_1$**; the emission peaks centered at 810 nm and 1270 are monitored. (D) Chemical structure of **Pyr$_1$RuPZn$_2$RuPyr$_1$**, and general experimental conditions; R group denotes 2'6'-bis(3,3-dimethyl-1butyloxy)phenyl.

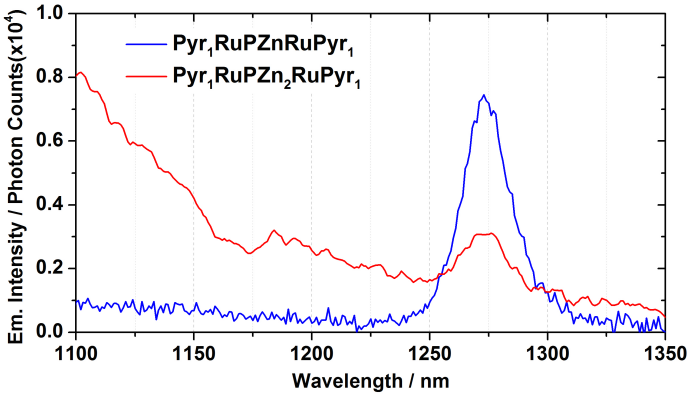

Figure S9. $O_2(^1\Delta)$ emission intensity comparison between **Pyr$_1$RuPZnRuPyr$_1$** and **Pyr$_1$RuPZn$_2$RuPyr$_1$**. Experimental conditions: ambient temperature; solvent = acetonitrile; λ_{exc} (**Pyr$_1$RuPZnRuPyr$_1$**) = λ_{exc} (**Pyr$_1$RuPZn$_2$RuPyr$_1$**) = 525 nm (O.D ~0.1 at 525 nm); samples were purged under air for ~30 min. Note that as the $O_2(^1\Delta)$ emission intensity is determined not only by the Φ_{ISC} of the sensitizer, but also by the sensitizer-to-oxygen

triplet energy transfer efficiency, this $O_2(^1\Delta)$ emission intensity comparison only qualitatively reflects relative **Pyr$_1$RuPZnRuPyr$_1$** and **Pyr$_1$RuPZn$_2$RuPyr$_1$** ISC efficiencies.

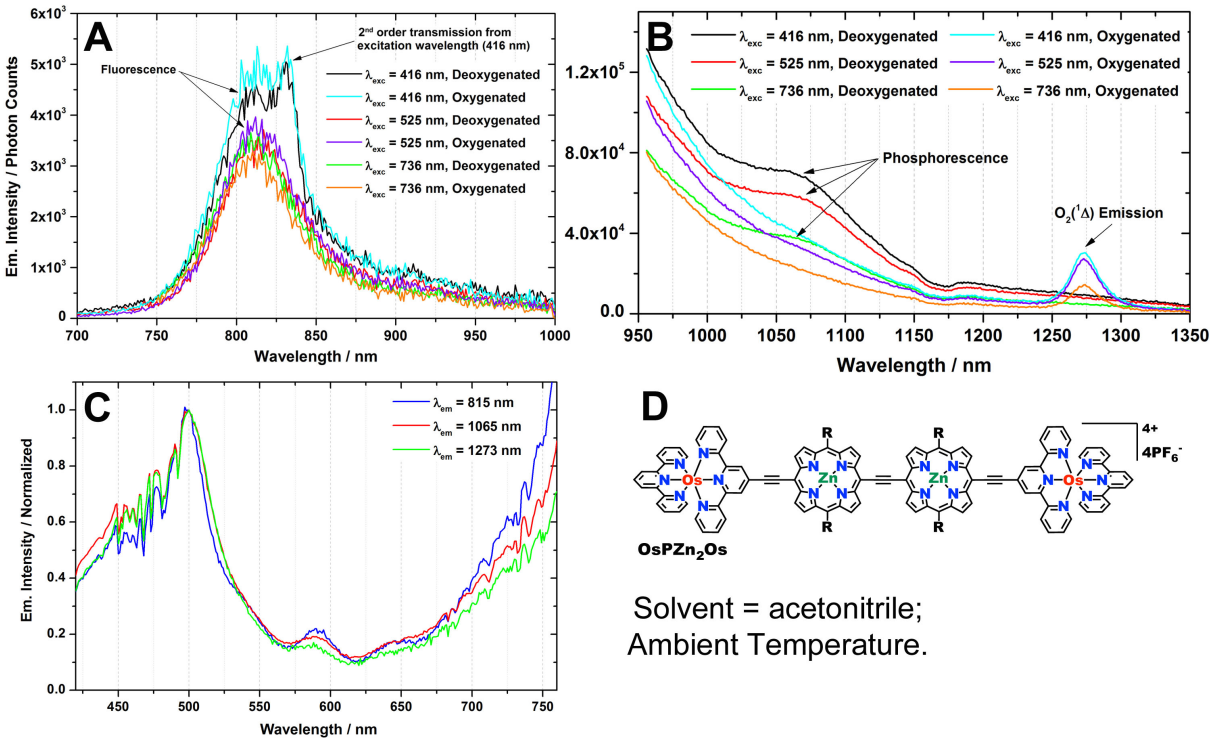

Figure S10. (A) and (B): **OsPZn$_2$Os** emission spectra taken under deoxygenated and oxygenated conditions, with peak assignments marked in the spectra; note that the phosphorescence signal appears on the tail of the fluorescence in (B). (C) Excitation scanning spectra for **OsPZn$_2$Os**; the emission peaks centered at 815 nm, 1065 nm, and 1273 nm are monitored. (D) Chemical structure of **OsPZn$_2$Os**, and general experimental conditions; R group denotes 2'6'-bis(3,3-dimethyl-1butyloxy)phenyl.

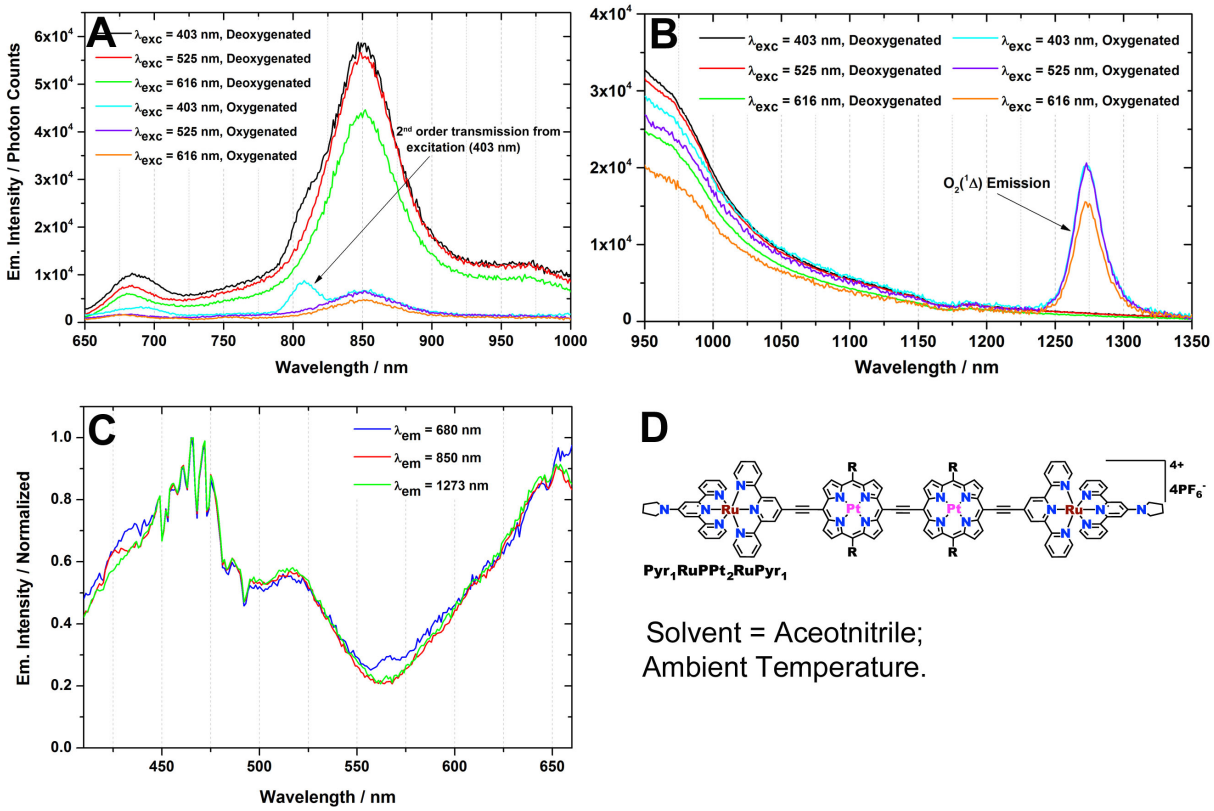

Figure S11. (A) and (B): **Pyr$_1$RuPPt$_2$RuPyr$_1$** emission spectra taken under deoxygenated and oxygenated conditions, with peak assignments marked in the spectra; note that based on the emission quenching behavior exhibited under oxygenated conditions, all the peaks in the spectra are assigned as phosphorescence (except for the one centered at ~806 nm due to 2nd order transmission from the excitation light source, and the one centered at ~1273 nm due to $O_2(^1\Delta)$ emission). (C) Excitation scanning spectra for **Pyr$_1$RuPPt$_2$RuPyr$_1$**; the emission peaks centered at 680 nm, 850 nm, and 1273 nm are monitored. (D) Chemical structure of **Pyr$_1$RuPPt$_2$RuPyr$_1$**, and general experimental conditions; R group denotes 2'6'-bis(3,3-dimethyl-1butyloxy)phenyl.

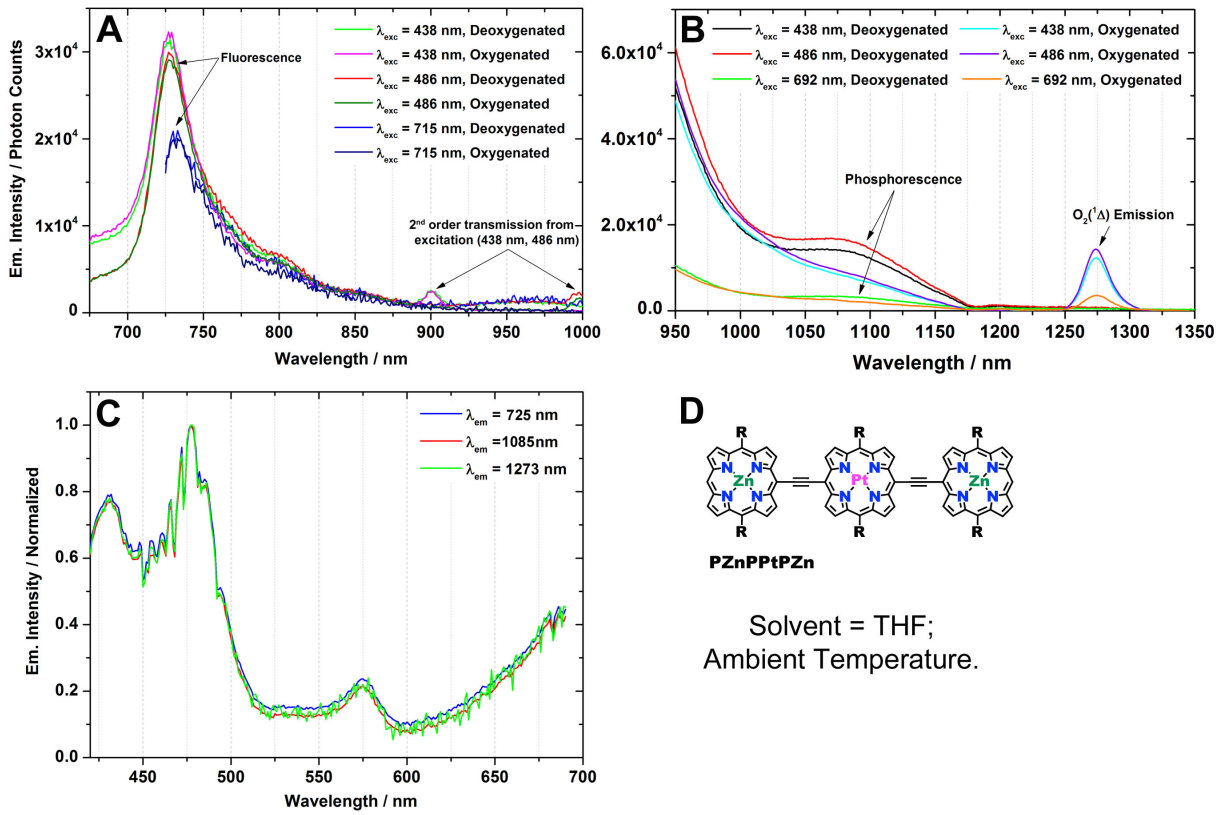

Figure S12. (A) and (B): **PZnPPtPZn** emission spectra taken under deoxygenated and oxygenated conditions, with peak assignments marked in the spectra; note that phosphorescence appears on the tail of the fluorescence in (B). (C) Excitation scanning spectra for **PZnPPtPZn**; the emission peaks centered at 725 nm, 1085 nm, and 1273 nm are monitored. (D) Chemical structure of **PZnPPtPZn**, and general experimental conditions; R group denotes 2'6'-bis(3,3-dimethyl-1butyloxy)phenyl.

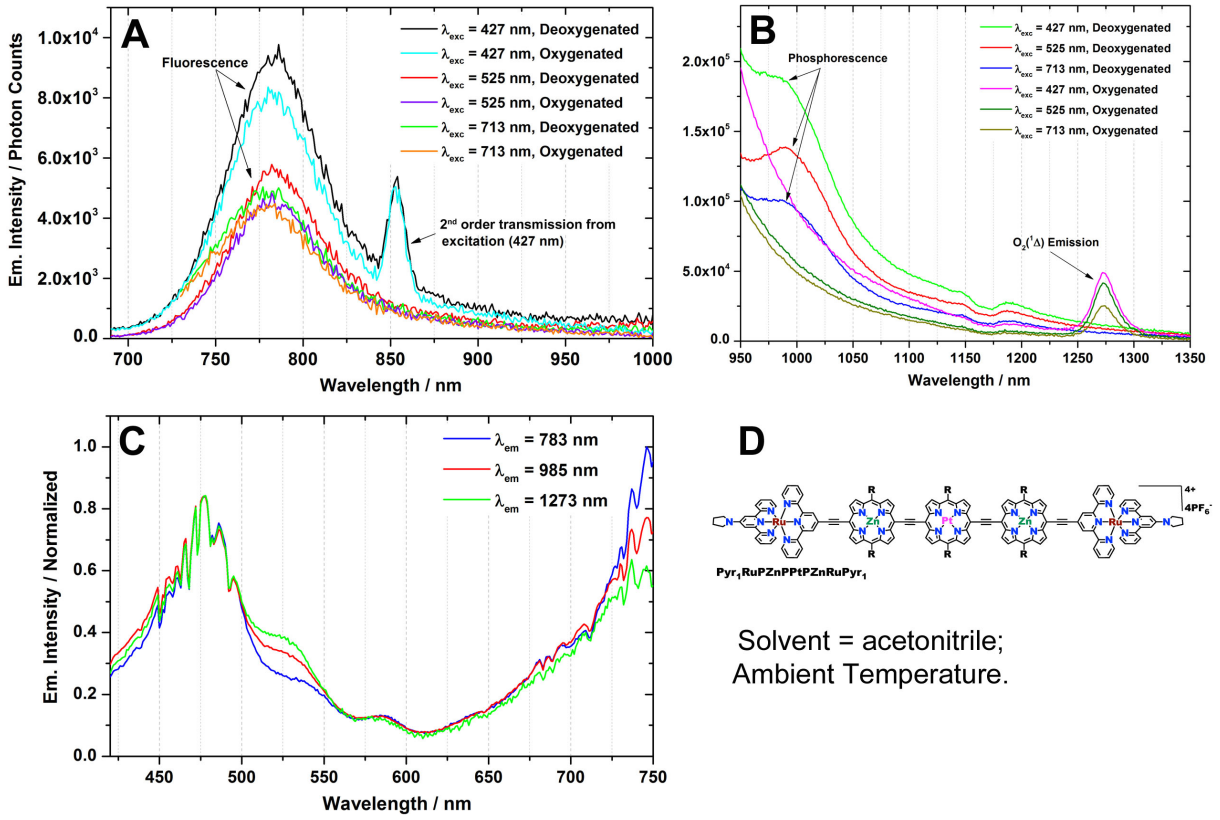

Figure S13. (A) and (B): **$Pyr_1RuPZnPPtPZnRuPyr_1$** emission spectra taken under deoxygenated and oxygenated conditions, with peak assignments marked in the spectra; note that phosphorescence appears on the tail of the fluorescence in (B). (C) Excitation scanning spectra for **$Pyr_1RuPZnPPtPZnRuPyr_1$**; the emission peaks centered at 783 nm, 985 nm, and 1273 nm are monitored. (D) Chemical structure of **$Pyr_1RuPZnPPtPZnRuPyr_1$**, and general experimental conditions; R group denotes 2'6'-bis(3,3-dimethyl-1butyloxy)phenyl.

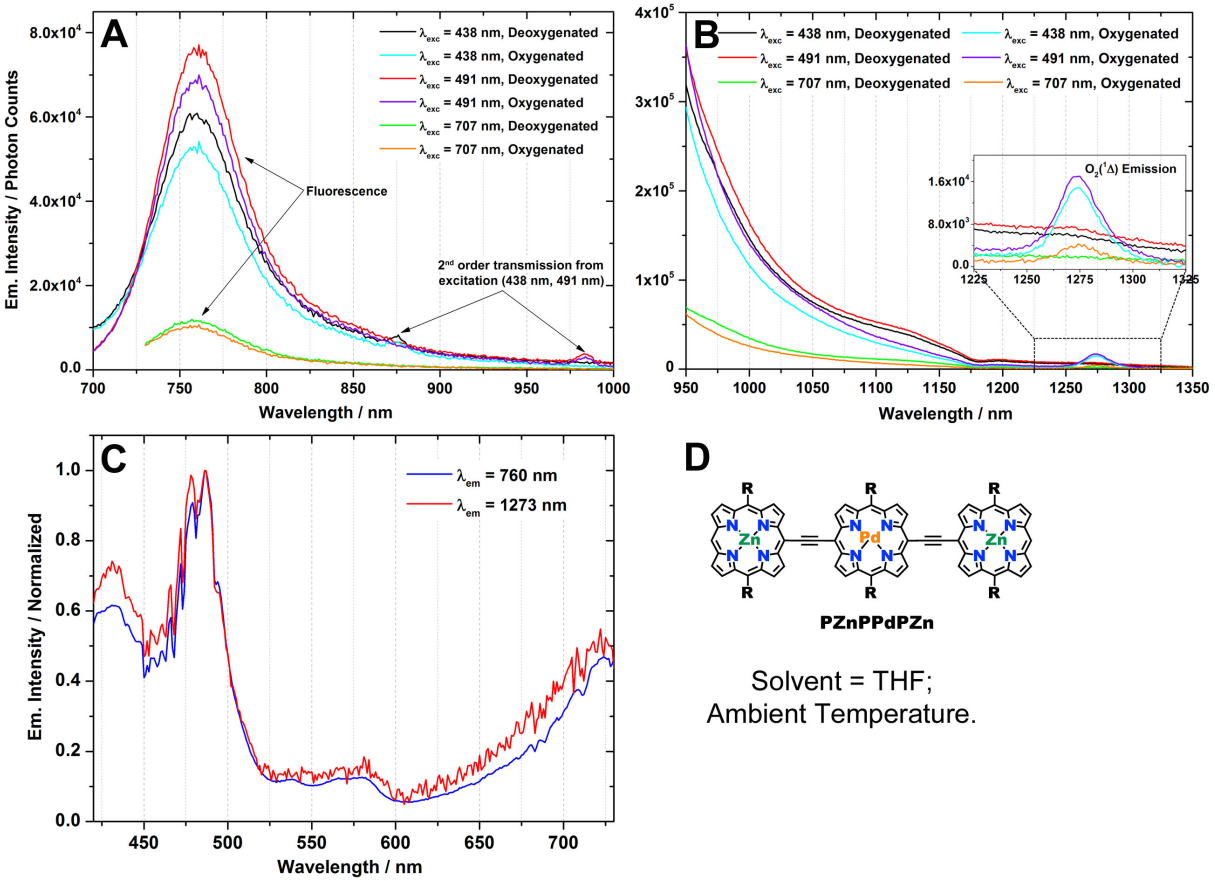

Figure S14. (A) and (B): **PZnPPdPZn** emission spectra taken under deoxygenated and oxygenated conditions, with peak assignments marked in the spectra. (C) Excitation scanning spectra for **PZnPPdPZn**; the emission peaks centered at 760 nm, and 1273 nm are monitored. (D) Chemical structure of **PZnPPdPZn**, and general experimental conditions; R group denotes 2'6'-bis(3,3-dimethyl-1butyloxy)phenyl.

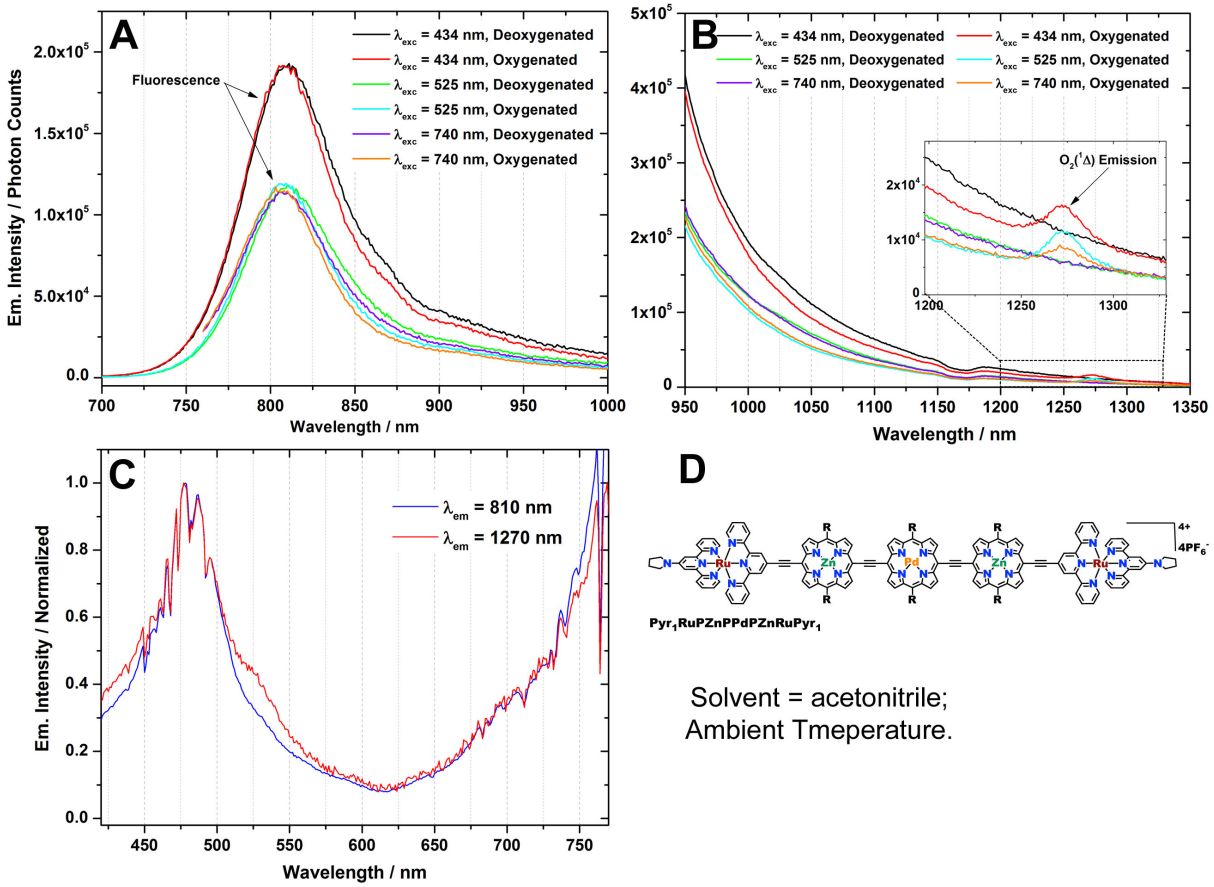

Figure S15. (A), and (B): **Pyr$_1$RuPZnPPdPZnRuPyr$_1$** emission spectra taken under deoxygenated and oxygenated conditions, with peak assignments marked in the spectra. (C) Excitation scanning spectra for **Pyr$_1$RuPZnPPdPZnRuPyr$_1$**; the emission peaks centered at 810 nm, and 1270 nm are monitored. (D) Chemical structure of **Pyr$_1$RuPZnPPdPZnRuPyr$_1$**, and general experimental conditions; R group denotes 2'6'-bis(3,3-dimethyl-1butyloxy)phenyl.

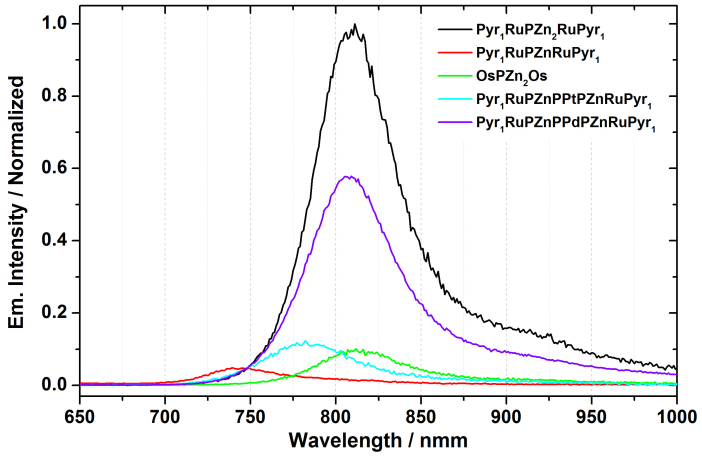

Figure S16. Fluorescence intensity comparison between **Pyr$_1$RuPZn$_2$RuPyr$_1$**, **Pyr$_1$RuPZnRuPyr$_1$**, **OsPZn$_2$Os**, **Pyr$_1$RuPZnPPtPZnRuPyr$_1$**, and **Pyr$_1$RuPZnPPdPZnRuPyr$_1$**. Spectra recorded under ambient conditions and

corrected for sample concentration; all chromophores here are excited at 525 nm (^{1}MLCT band) in acetonitrile solvent.

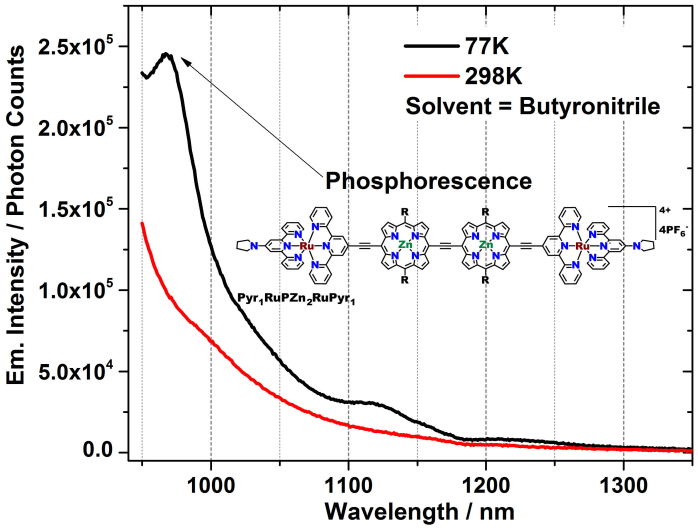

Figure S17. NIR photoluminescence spectra of **Pyr$_1$RuPZn$_2$RuPyr$_1$**, measured at low temperature (77K) and room temperature (298K). Experimental conditions: λ_{Exc} = 525 nm (^{1}MLCT band), solvent = butyronitrile; prior to these measurements, the sample was subject to three freeze-pump-thaw-degas cycles.

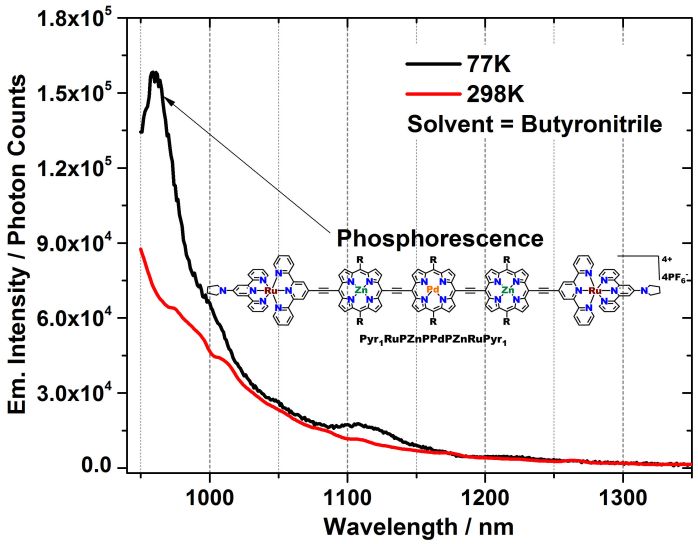

Figure S18. NIR photoluminescence spectra of **Pyr$_1$PZnPPdPZnPyr$_1$**, measured at low temperature (77K) and room temperature (298K). Experimental conditions: λ_{Exc} = 525 nm (^{1}MLCT band), solvent = butyronitrile; prior to these measurements, the sample was subject to three freeze-pump-thaw-degas cycles.

4. Picosecond Fluorescence Lifetime Results

The fluorescence lifetimes of all chromophores were measured in acetonitrile solvent under ambient conditions (note that the extremely weak fluorescence intensity and short S_1 state lifetime of **Pyr$_1$RuPZnRuPyr$_1$** precluded a fluorescence lifetime determination by the streak camera exploited here).

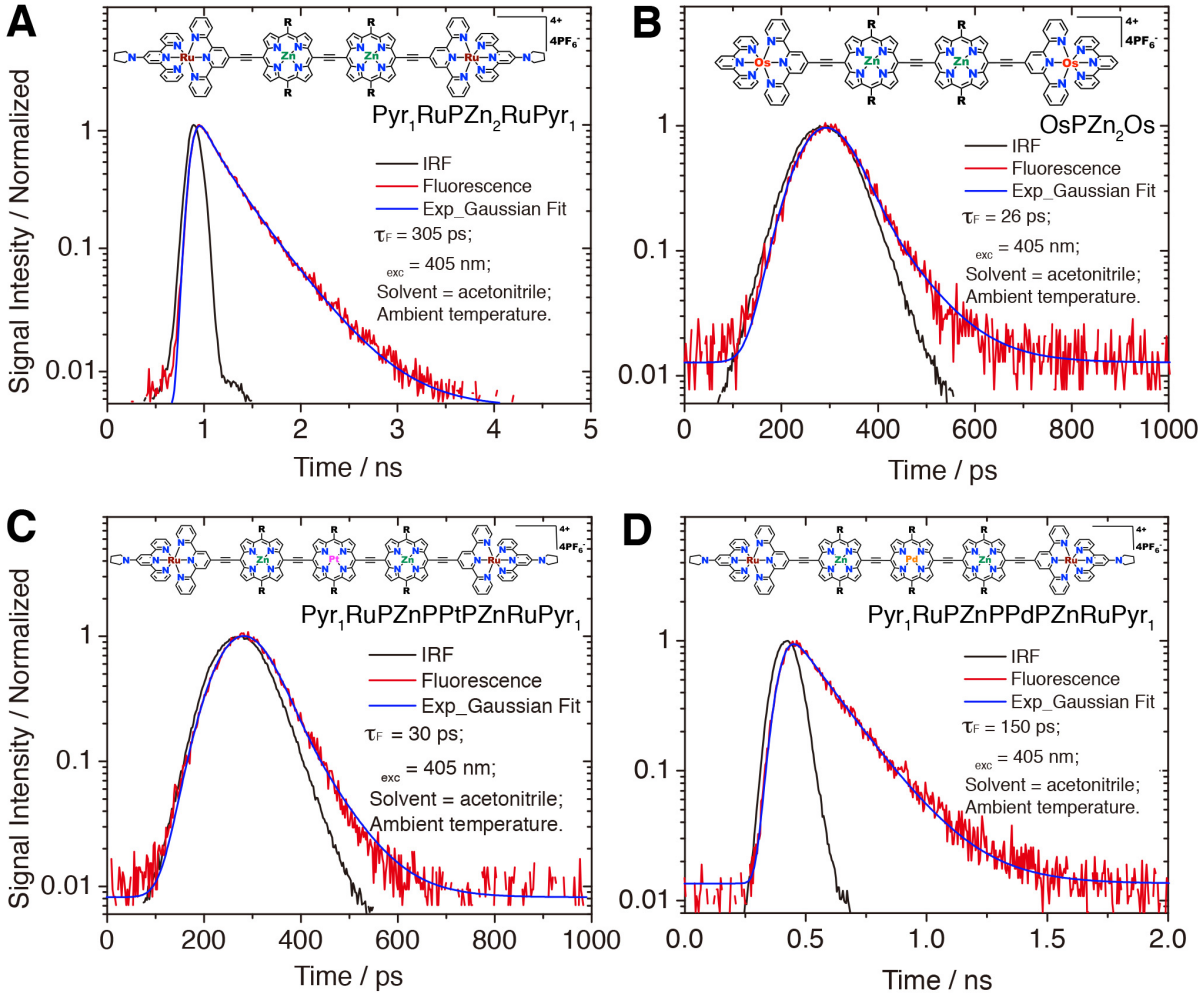

Figure S19. Picosecond timescale fluorescence decays determined for: (A) **Pyr$_1$RuPZn$_2$RuPyr$_1$**, (B) **OsPZn$_2$Os**, (C) **Pyr$_1$RuPZnPPtPZnRuPyr$_1$**, and (D) **Pyr$_1$RuPZnPPdPZnRuPyr$_1$**. Instrument response function and fluorescence decay are plotted in black and red solid lines, respectively. Data fitting was accomplished with Gaussian-exponential convoluted functions. Experimental conditions: λ_{exc} = 405 nm, solvent = MeCN, ambient temperature.

5. Nanosecond-to-Microsecond Transient Absorption

Nanosecond-to-microsecond timescale transient absorption spectra for all chromophores were recorded using an air-free spectro-cell; prior to these measurements, all samples were subject to three freeze-pump-thaw-degas cycles. When necessary, sample oxygenation was achieved by purging with air for ~30 min before measurements. Kinetic data were fitted with single-exponential decay functions to acquire the triplet excited state lifetimes.

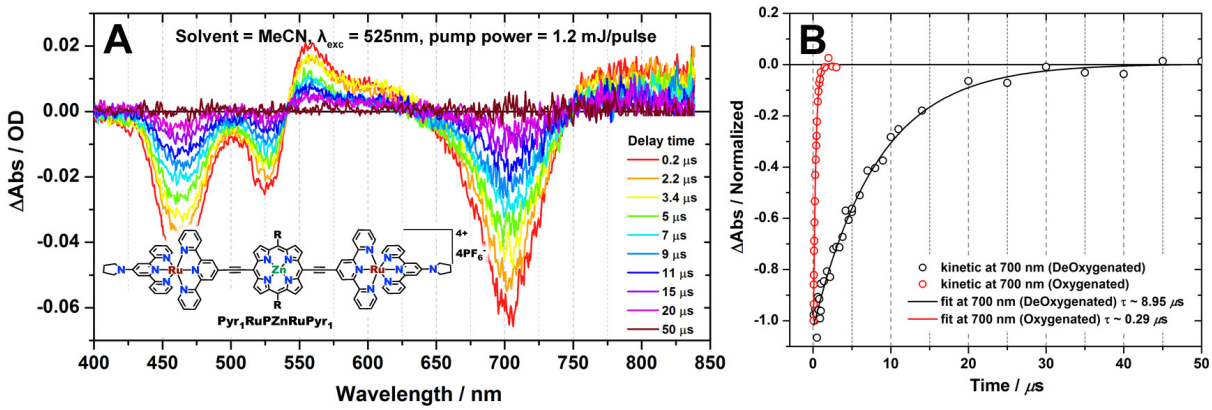

Figure S20. (A) Nanosecond-to-microsecond transient absorption spectra recorded at selected time delays for **Pyr$_1$RuPZnRuPyr$_1$**. Experimental conditions: λ_{exc} = 525 nm, pump power = 1.2 mJ / pulse, solvent = MeCN, deoxygenated, ambient temperature. (B) Nanosecond-to-microsecond transient kinetic traces recorded at 700 nm for **Pyr$_1$RuPZnRuPyr$_1$** under deoxygenated and oxygenated conditions, respectively. Experimental conditions: λ_{exc} = 525 nm, pump power = 1.2 mJ / pulse, solvent = MeCN, ambient temperature.

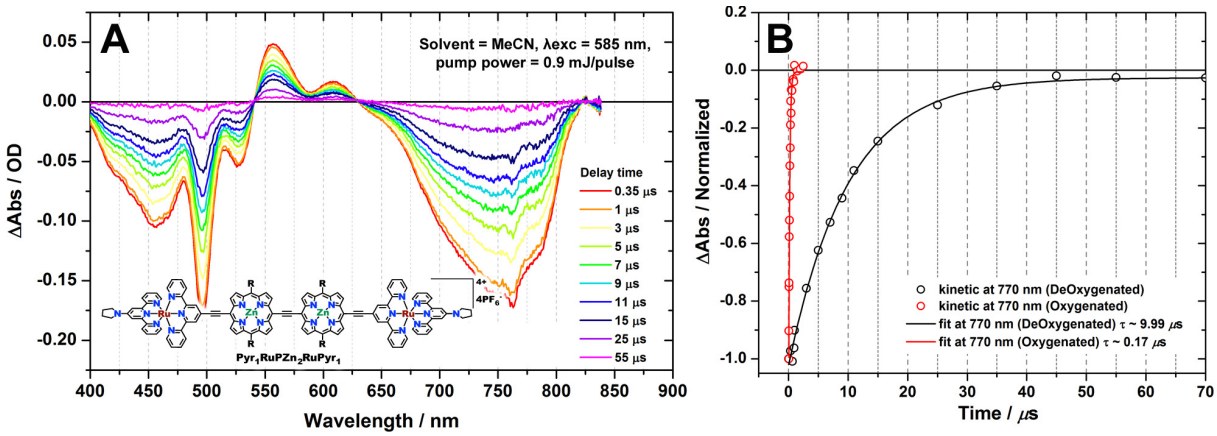

Figure S21. (A) Nanosecond-to-microsecond transient absorption spectra recorded at selected time delays for **Pyr$_1$RuPZn$_2$RuPyr$_1$**. Experimental conditions: λ_{exc} = 585 nm, pump power = 0.9 mJ / pulse, solvent = MeCN, deoxygenated, ambient temperature. (B) Nanosecond-to-microsecond transient kinetic traces recorded at 770 nm for **Pyr$_1$RuPZn$_2$RuPyr$_1$** under deoxygenated and oxygenated conditions, respectively. Experimental conditions: λ_{exc} = 585 nm, pump power = 0.9 mJ / pulse, solvent = MeCN, ambient temperature.

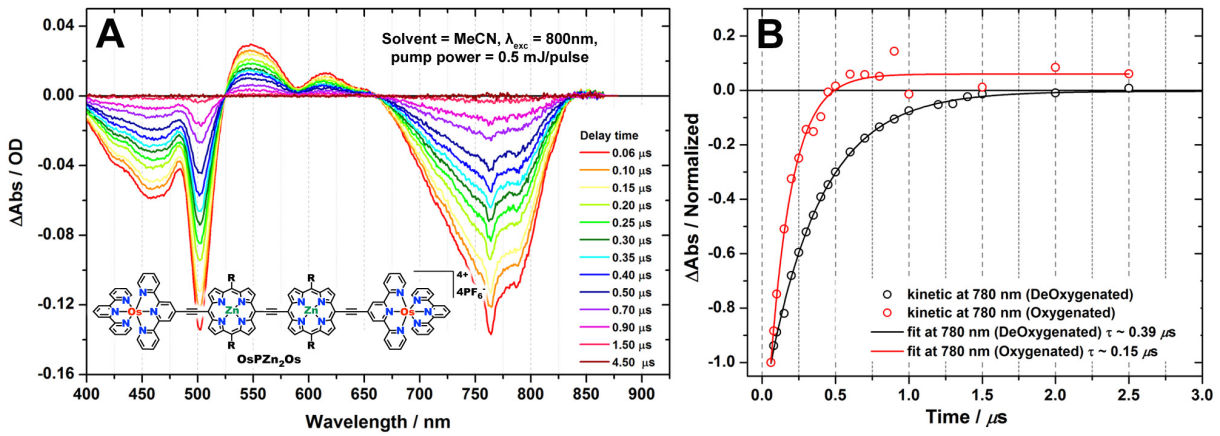

Figure S22. (A) Nanosecond-to-microsecond transient absorption spectra recorded at selected time delays for **OsPZn$_2$Os**. Experimental conditions: λ_{exc} = 800 nm, pump power = 0.5 mJ / pulse, solvent = MeCN, deoxygenated, ambient temperature. (B) Nanosecond-to-microsecond transient kinetic traces recorded at 780 nm for **OsPZn$_2$Os** under deoxygenated and oxygenated conditions, respectively. Experimental conditions: λ_{exc} = 800 nm, pump power = 0.5 mJ / pulse, solvent = MeCN, ambient temperature.

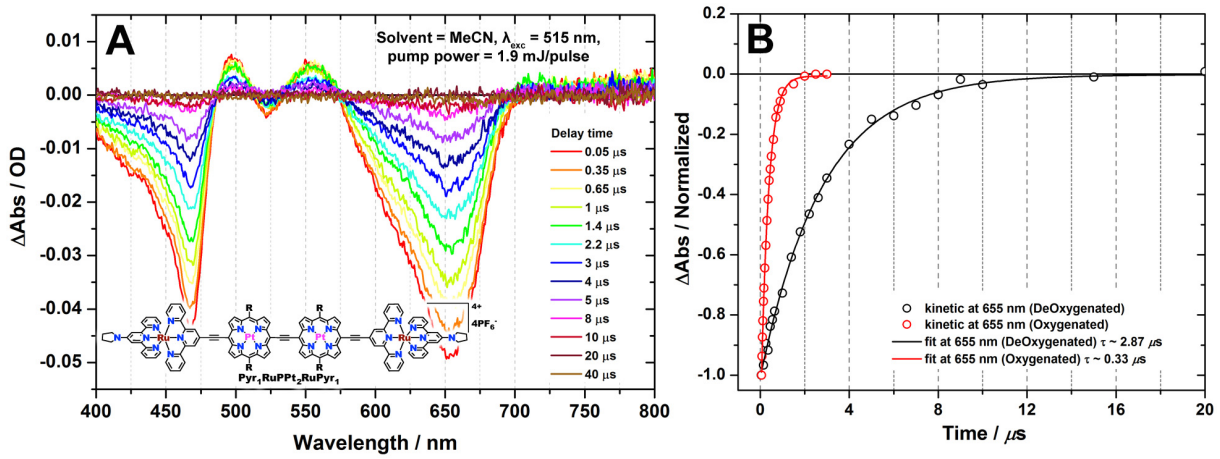

Figure S23. (A) Nanosecond-to-microsecond transient absorption spectra recorded at selected time delays for **Pyr$_1$RuPPt$_2$RuPyr$_1$**. Experimental condition: λ_{exc} = 515 nm, pump power = 1.9 mJ / pulse, solvent = MeCN, deoxygenated, ambient temperature. (B) Nanosecond-to-microsecond transient kinetic traces recorded at 655 nm for **Pyr$_1$RuPPt$_2$RuPyr$_1$** under deoxygenated and oxygenated condition, respectively. Experimental condition: λ_{exc} = 515 nm, pump power = 1.9 mJ / pulse, solvent = MeCN, ambient temperature.

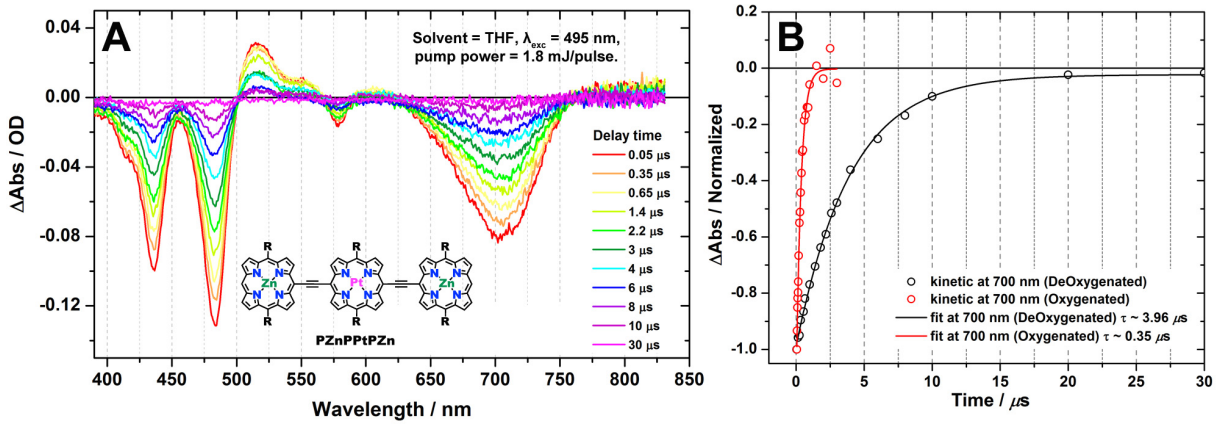

Figure S24. (A) Nanosecond-to-microsecond transient absorption spectra recorded at selected time delays for **PZnPPtPZn**. Experimental conditions: λ_{exc} = 495 nm, pump power = 1.8 mJ / pulse, solvent = THF, deoxygenated, ambient temperature. (B) Nanosecond-to-microsecond transient kinetic traces recorded at 700 nm for **PZnPPtPZn** under deoxygenated and oxygenated conditions, respectively. Experimental condition: λ_{exc} = 495 nm, pump power = 1.8 mJ / pulse, solvent = THF, ambient temperature.

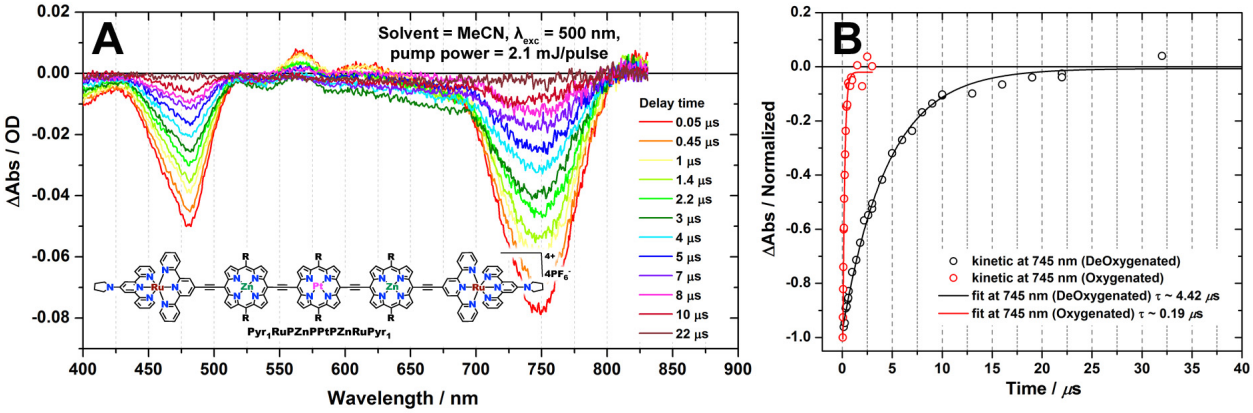

Figure S25. (A) Nanosecond-to-microsecond transient absorption spectra recorded at selected time delays for **Pyr_1RuPZnPPtPZnRuPyr_1**. Experimental conditions: λ_{exc} = 500 nm, pump power = 2.1 mJ / pulse, solvent = MeCN, deoxygenated, ambient temperature. (B) Nanosecond-to-microsecond transient kinetic traces recorded at 745 nm for **Pyr_1RuPZnPPtPZnRuPyr_1** under deoxygenated and oxygenated conditions, respectively. Experimental conditions: λ_{exc} = 500 nm, pump power = 2.1 mJ / pulse, solvent = MeCN, ambient temperature.

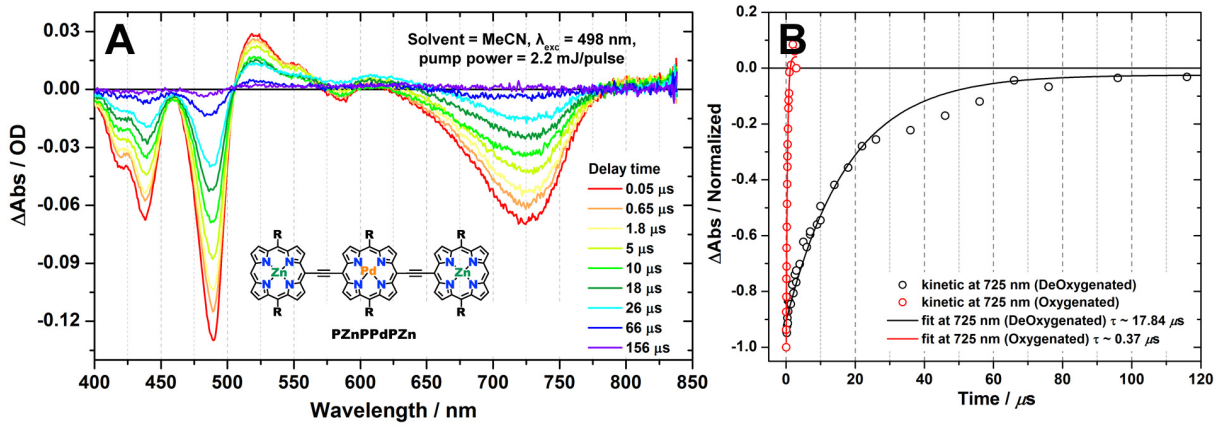

Figure S26. (A) Nanosecond-to-microsecond transient absorption spectra recorded at selected time delays for **PZnPPdPZn**. Experimental conditions: λ_{exc} = 498 nm, pump power = 2.2 mJ / pulse, solvent = THF, deoxygenated, ambient temperature. (B) Nanosecond-to-microsecond transient kinetic traces recorded at 725 nm for **PZnPPdPZn** under deoxygenated and oxygenated conditions, respectively. Experimental conditions: λ_{exc} = 498 nm, pump power = 2.2 mJ / pulse, solvent = THF, ambient temperature.

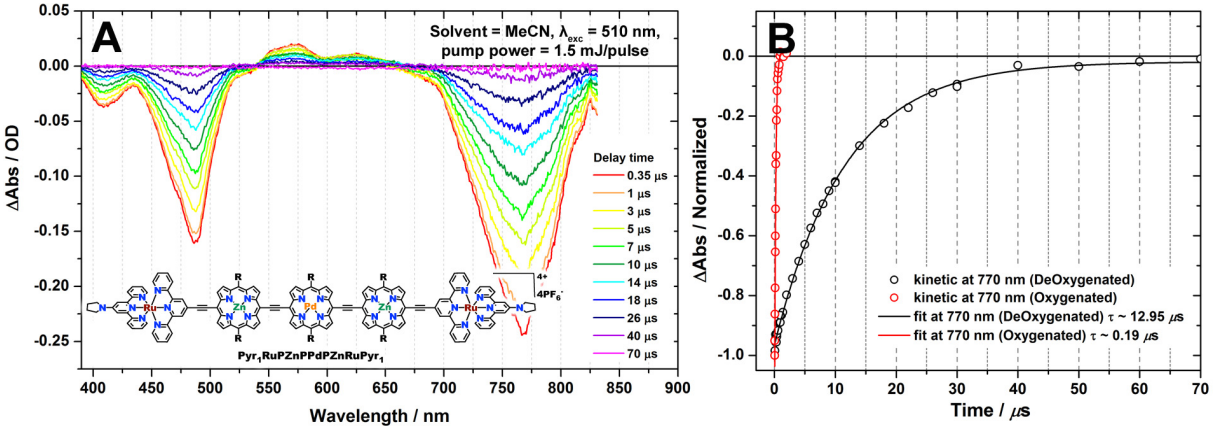

Figure S27. (A) Nanosecond-to-microsecond transient absorption spectra recorded at selected time delays for **Pyr_1RuPZnPPdPZnRuPyr_1**. Experimental conditions: λ_{exc} = 510 nm, pump power = 1.5 mJ / pulse, solvent = MeCN, deoxygenated, ambient temperature. (B) Nanosecond-to-microsecond transient kinetic traces recorded at 770 nm for **Pyr_1RuPZnPPdPZnRuPyr_1** under deoxygenated and oxygenated conditions, respectively. Experimental conditions: λ_{exc} = 510 nm, pump power = 1.5 mJ / pulse, solvent = MeCN, ambient temperature.

6. Other Supplementary Spectroscopic Data

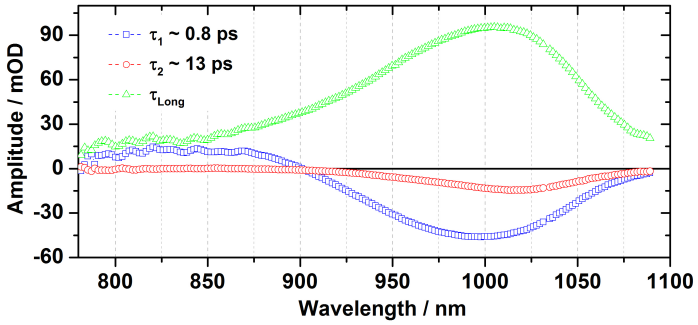

Figure S28. DADS of the NIR regime, revealing near-unit *ISC* processes and the torsional dynamics for **Pyr$_1$RuPZnRuPyr$_1$**. The negative amplitude on the red side (900 – 1100 nm) accounts for $S_1 \rightarrow T_1$ *ISC* process (~0.8 ps) and torsional dynamics (~13 ps), respectively. On the blue side (780 – 900 nm), the 13 ps component displays zero amplitude, whereas the 0.8 ps component is positive, representing the S_1 state decay process. The long-lived component accounts for the decay of the evolved excited triplet states, which persists beyond the limit of the fs pump-probe delay limit.

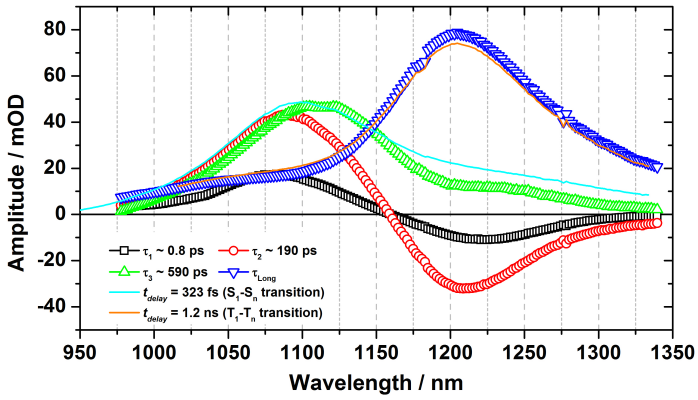

Figure S29. DADS of NIR regime for **Pyr$_1$RuPZn$_2$RuPyr$_1$**. Four decay components are evident in this spectral region: a long-lived component that overlaps with the $T_1 \rightarrow T_n$ transition and represents the slow decay process of the excited triplet state; an s-like component with a time constant of ~0.8 ps that corresponds to the solvent dynamics; another s-like component with a time constant of ~190 ps that represents conformational relaxation the and $S_1 \rightarrow T_1$ ISC processes; the last component of ~590 ps that overlaps with the $S_1 \rightarrow S_n$ transition accounts for non-radiative or processes that depopulate the S_1 state.

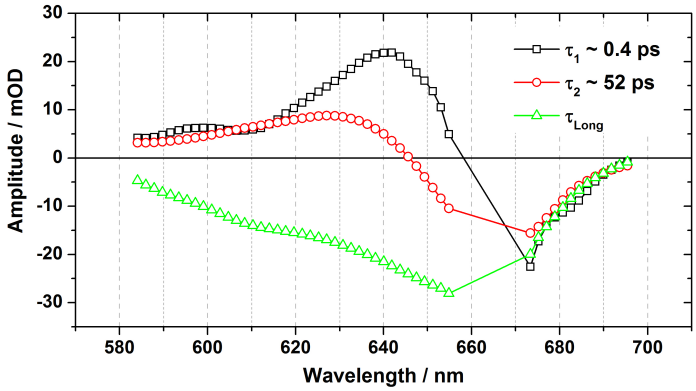

Figure S30. DADS of the *Q*-band region for **Pyr$_1$RuPPt$_2$RuPyr$_1$**. Due to excitation light scattering, the signal between 655 and 671 nm was removed from the spectra. Note that a component of ~52 ps is evinced that displays positive amplitude on the blue side and negative on the red side, resulting in spectra broadening and a slight blue shift of the *Q*-band bleach over this time domain. This component (52 ps) is also observed in the *Q*-band DADS of **Pyr$_1$RuPZn$_2$RuPyr$_1$** and originates from conformational heterogeneity and spectral diffusion following photoexcitation.

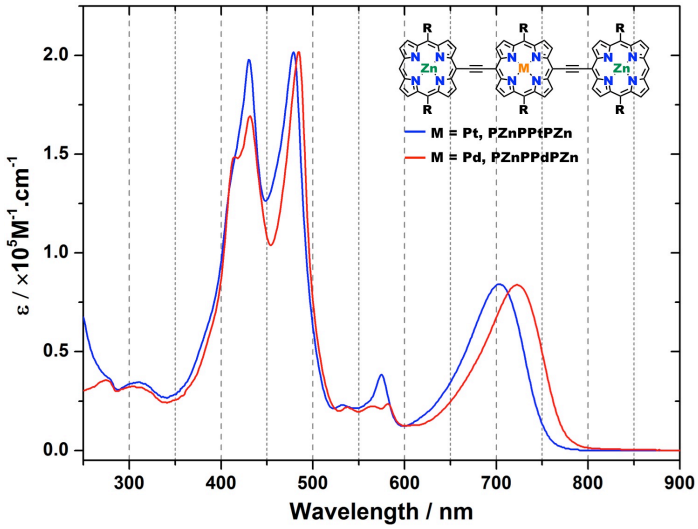

Figure S31. Electronic absorption spectra of **PZnPPtPZn** (blue solid line) and **PZnPPdPZn** (red solid line). These spectra were recorded under ambient conditions in THF solvent. R group represents 2'6'-bis(3,3-dimethyl-1butyloxy)phenyl.

7. TD-DFT Calculations and Population Analyses Performed for Oligo(Porphinato)Metal(II) Species

All calculations were performed upon structures with aliphatic chains truncated to methyl groups (Figure S32, molecular structures shown at the top of the figure). For these oligo(porphinato)metal(II) species, C_{2v} conformeric minima could be formulated. Ground-state structure optimizations were performed with Density Functional Theory (DFT) using Gaussian 09, Rev C.1.[5] The Becke three-parameter hybrid[6] and the Lee-Yang-Parr correlation functional[7] were employed for all calculations (B3LYP). Optimizations were performed with minimal symmetry constraints using tight optimization criteria; initial optimizations used smaller basis sets but the final optimizations and TD-DFT calculations employed the 6-311g(d) basis set as implemented in Gaussian 09. TD-DFT result files were post-processed using the GaussSum package;[8] this software partitions the wavefunction amplitudes onto molecule fragments using Mulliken population analysis.[9]

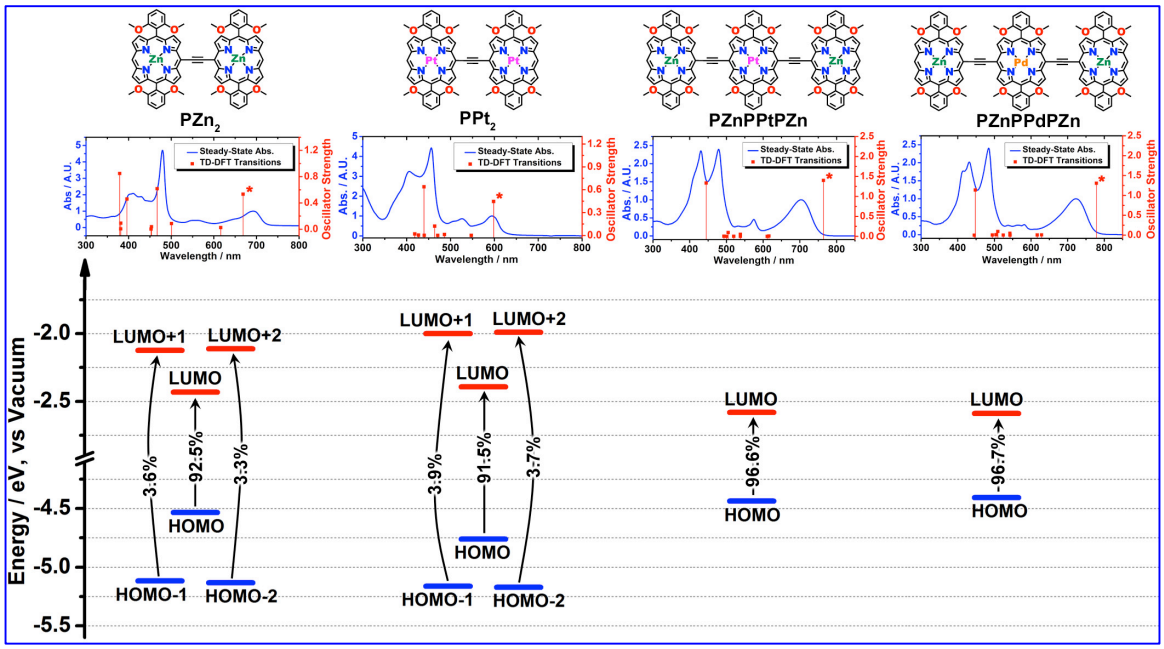

Figure S32. Molecular structures of oligo(porphinato)metal(II) and TD-DFT determined one-electron configurations depicted as arrows with percentages representing the major excitation's contribution to the low-lying excited-state transition (marked as " * " in the middle spectral figures) for oligo(porphinato)metal(II) structures. TD-DFT predicted transitions and the corresponding oscillator strength are plotted with experimentally measured ground-state absorption for comparison (middle figures).

Table S1. Mulliken Population Analysis on **PPt_2** (Chemical Formula: **$C_{74}H_{54}N_8O_8Pt_2$**) Highlighting Wavefunction Amplitudes Partitioned onto Platinum Atoms.

Orbitals	Energy / eV	Symmetry	Groups / Atoms (percentage contribution to MO, %)	
			$C_{74}H_{54}N_8O_8$	Pt_2
L+2	-1.99	A2	96.7	3.3
L+1	-2	B1	96.7	3.3
LUMO	-2.39	B2	97.1	2.9
HOMO	-4.76	A1	98.7	1.3
H-1	-5.16	A2	99.9	0.1
H-2	-5.17	B1	99.9	0.1

Table S2. Mulliken Population Analysis on **PZn_2** (Chemical Formula: **$C_{74}H_{54}N_8O_8Zn_2$**) Highlighting Wavefunction Amplitudes Partitioned onto Zinc Atoms.

Orbitals	Energy / eV	Symmetry	Groups / Atoms (percentage contribution to MO, %)	
			$C_{74}H_{54}N_8O_8$	Zn_2
L+2	-2.01	A2	99.9	0.1
L+1	-2.02	B1	99.9	0.1
LUMO	-2.4	B2	99.7	0.3
HOMO	-4.53	A1	97.8	2.2
H-1	-5.04	A2	100.0	0.0
H-2	-5.05	B1	100.0	0.0

Table S3. Mulliken Population Analysis on **PZnPPtPZn** (Chemical Formula: **$C_{112}H_{80}N_{12}O_{12}Zn_2Pt$**) Highlighting Wavefunction Amplitudes Partitioned onto Zinc and Platinum Atoms.

Orbitals	Energy / eV	Symmetry	Groups / Atoms (percentage contribution to MO, %)		
			$C_{112}H_{80}N_{12}O_{12}$	Zn_2	Pt
L+2	-2.04	A2	99.9	0.1	0.0
L+1	-2.16	B1	99.8	0.1	0.1
LUMO	-2.54	B1	98.5	0.2	1.3
HOMO	-4.49	B1	98.2	1.2	0.6
H-1	-4.89	B1	98.0	2.0	0.0
H-2	-5.07	A2	100.0	0.0	0.0

Table S4. Mulliken Population Analysis on **PZnPPdPZn** (Chemical Formula: **$C_{112}H_{80}N_{12}O_{12}Zn_2Pd$**) Highlighting Wavefunction Amplitudes Partitioned onto Zinc and Palladium Atoms

Orbitals	Energy / eV	Symmetry	Groups / Atoms (percentage contribution to MO, %)		
			$C_{112}H_{80}N_{12}O_{12}$	Zn_2	Pd
L+2	-2.04	A2	99.9	0.1	0.0
L+1	-2.15	B1	99.8	0.1	0.1
LUMO	-2.55	B1	99.1	0.2	0.7
HOMO	-4.45	B1	98.2	1.2	0.6
H-1	-4.88	B1	98.0	2.0	0.0
H-2	-5.07	A2	100.0	0.0	0.0

References:

(1) (a) Constable, E. C.; Thompson, A. M. W. C. *J. Chem. Soc., Dalton Trans.* **1995**, 1615-1627. (b) Constable, E. C.; Ward, M. D. *J. Chem. Soc., Dalton Trans.* **1990**, 1405-1409. (c) Potts, K. T.; Konwar, D. *J. Org. Chem.* **1991**, *56*, 4815-4816. (d) Holbrey, J. D.; Tiddy, G. J. T.; Bruce, D. W. *J. Chem. Soc., Dalton Trans.* **1995**, 1769-1774. (e) Duncan, T. V.; Ishizuka, T.; Therien, M. J. *J. Am. Chem. Soc.* **2007**, *129*, 9691-9703. (f) Adcock, P. A.; Keene, F. R.; Smythe, R. S.; Snow, M. R. *Inorg. Chem.* **1984**, *23*, 2336-2343. (g) Kober, E. M.; Marshall, J. L.; Dressick, W. J.; Sullivan, B. P.; Caspar, J. V.; Meyer, T. J. *Inorg. Chem.* **1985**, *24*, 2755-2763. (h) Coe, B. J.; Thompson, D. W.; Culbertson, C. T.; Schoonover, J. R.; Meyer, T. J. *Inorg. Chem.* **1995**, *34*, 3385-3395.

(2) (a) Uyeda, H. T.; Zhao, Y. X.; Wostyn, K.; Asselberghs, I.; Clays, K.; Persoons, A.; Therien, M. J. *J. Am. Chem. Soc.* **2002**, *124*, 13806-13813. (b) Barigelletti, F.; Flamigni, L.; Balzani, V.; Collin, J.-P.; Sauvage, J.-P.; Sour, A.; Constable, E. C.; Thompson, A. M. W. C. *J. Am. Chem. Soc.* **1994**, *116*, 7692-7699. (c) Brewer, R. G.; Jensen, G. E.; Brewer, K. J. *Inorg. Chem.* **1994**, *33*, 124-129. (d) Vogler, L. M.; Brewer, K. J. *Inorg. Chem.* **1996**, *35*, 818-824.

(3) Susumu, K.; Therien, M. J. *J. Am. Chem. Soc.* **2002**, *124*, 8550-8552.

(4) Duncan, T. V.; Frail, P. R.; Miloradovic, I. R.; Therien, M. J. *J. Phys. Chem. B* **2010**, *114*, 14696-14702.

(5) Frisch, M. J.; Trucks, G. W.; Schlegel, H. B.; Scuseria, G. E.; Robb, M. A.; Cheeseman, J. R.; Scalmani, G.; Barone, V.; Mennucci, B.; Petersson, G. A.; Nakatsuji, H.; Caricato, M.; Li, X.; Hratchian, H. P.; Izmaylov, A. F.; Bloino, J.; Zheng, G.; Sonnenberg, J. L.; Hada, M. E., M.; Toyota, K.; Fukuda, R.; Hasegawa, J.; Ishida, M.; Nakajima, T.; Honda, Y.; Kitao, O.; Nakai, H.; Vreven, T.; Montgomery, J. A.; Peralta, J. E.; Ogliaro, F.; Bearpark, M.; Heyd, J. J.; Brothers, E.; Kudin, K. N.; Staroverov, V. N.; Kobayashi, R.; Normand, J.; Raghavachari, K.; Rendell, A.; Burant, J. C.; Iyengar, S. S.; Tomasi, J.; Cossi, M.; Rega, N.; Millam, J. M.; Klene, M.; Knox, J. E.; Cross, J. B.; Bakken, V.; Adamo, C.; Jaramillo, J.; Gomperts, R.; Stratmann, R. E.; Yazyev, O.; Austin, A. J.; Cammi, R.; Pomelli, C.; Ochterski, J. W.; Martin, R. L.; Morokuma, K.; Zakrzewski, V. G.; Voth, G. A.; Salvador, P.; Dannenberg, J. J.; Dapprich, S.; Daniels, A. D.; Farkas, Ö.; Foresman, J. B.; Ortiz, J. V.; Cioslowski, J.; Fox, D. J.; Rev. C.1. ed.; Gaussian, Inc.: Wallingford CT, 2009.

(6) Raghavachari, K. *Theor. Chem. Acc.* **2000**, *103*, 361-363.

(7) (a) Lee, C.; Yang, W.; Parr, R. G. *Phys. Rev. B* **1988**, *37*, 785-789. (b) Miehlich, B.; Savin, A.; Stoll, H.; Preuss, H. *Chem. Phys. Lett.* **1989**, *157*, 200-206.

(8) O'Boyle, N. M.; Tenderholt, A. L.; Langner, K. M. *J. Comput. Chem.* **2008**, *29*, 839-845.

(9) Mulliken, R. S. *J. Chem. Phys.* **1955**, *23*, 1833-1840.